

# Chemistry, Biosynthesis, Physicochemical and Biological Properties of Rubiadin: A Promising Natural Anthraquinone for New Drug Discovery and Development

Mohd Nasarudin Watroly,<sup>1</sup> Mahendran Sekar,<sup>1</sup> Shivkanya Fuloria,<sup>2</sup> Siew Hua Gan,<sup>3</sup> Srikanth Jeyabalan,<sup>4</sup> Yuan Seng Wu,<sup>5,6</sup> Vetriselvan Subramaniam,<sup>7</sup> Kathiresan V Sathasivam,<sup>8</sup> Subban Ravi,<sup>9</sup> Nur Najihah Izzati Mat Rani,<sup>10</sup> Pei Teng Lum,<sup>1</sup> Jaishree Vajjanathappa,<sup>11</sup> Dhanalekshmi Unnikrishnan Meenakshi,<sup>12</sup> Shankar Mani,<sup>13</sup> Neeraj Kumar Fuloria<sup>2</sup>

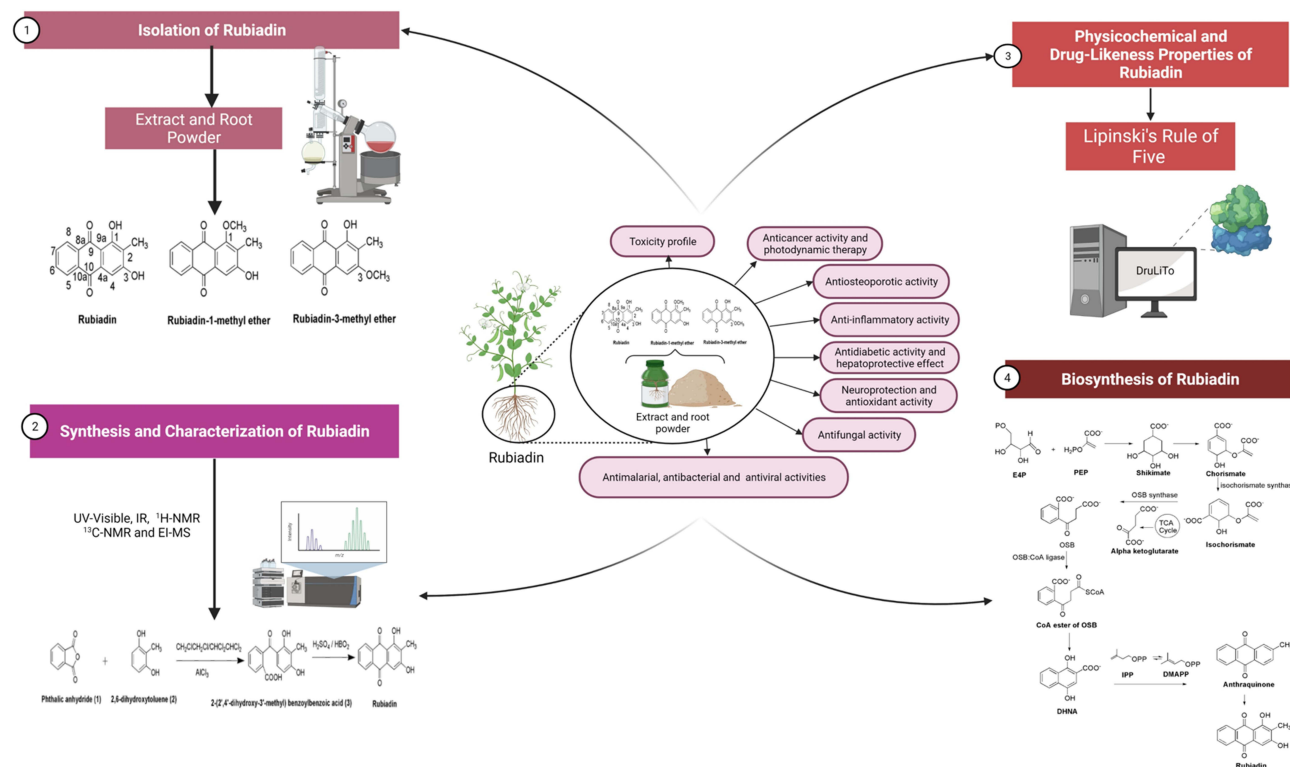
<sup>1</sup>Department of Pharmaceutical Chemistry, Faculty of Pharmacy and Health Sciences, Universiti Kuala Lumpur Royal College of Medicine Perak, Ipoh, Perak, 30450, Malaysia; <sup>2</sup>Faculty of Pharmacy & Centre of Excellence for Biomaterials Engineering, AIMST University, Kedah, 08100, Malaysia; <sup>3</sup>School of Pharmacy, Monash University Malaysia, Bandar Sunway, Selangor Darul Ehsan, 47500, Malaysia; <sup>4</sup>Department of Pharmacology, Sri Ramachandra Faculty of Pharmacy, Sri Ramachandra Institute of Higher Education and Research (DU), Chennai, Tamil Nadu, 600116, India; <sup>5</sup>Centre for Virus and Vaccine Research, School of Medical and Life Sciences, Sunway University, Selangor, 47500, Malaysia; <sup>6</sup>Department of Biological Sciences, School of Medical and Life Sciences, Sunway University, Selangor, 47500, Malaysia; <sup>7</sup>Faculty of Medicine, Bioscience and Nursing, MAHSA University, Selangor, 42610, Malaysia; <sup>8</sup>Faculty of Applied Science & Centre of Excellence for Biomaterials Engineering, AIMST University, Kedah, 08100, Malaysia; <sup>9</sup>Department of Chemistry, Karpagam Academy of Higher Education, Coimbatore, Tamil Nadu, 640 021, India; <sup>10</sup>Faculty of Pharmacy and Health Sciences, Universiti Kuala Lumpur Royal College of Medicine Perak, Ipoh, Perak, 30450, Malaysia; <sup>11</sup>Department of Pharmaceutical Chemistry, School of Life Sciences, JSS Academy of Higher Education and Research Mauritius, Vacoas, Mauritius; <sup>12</sup>College of Pharmacy, National University of Science and Technology, Muscat, 130, Oman; <sup>13</sup>Department of Pharmaceutical Chemistry, Sri Adichunchanagiri College of Pharmacy, Adichunchanagiri University, Mandya, Karnataka, 571418, India

Correspondence: Neeraj Kumar Fuloria; Shivkanya Fuloria  
Faculty of Pharmacy & Centre of Excellence for Biomaterials Engineering, AIMST University, Kedah, 08100, Malaysia  
Tel +60 16 4037685; +60 14 3034057  
Email neerajkumar@aimst.edu.my; shivkanya\_fuloria@aimst.edu.my

**Abstract:** Anthraquinones (AQs) are found in a variety of consumer products, including foods, nutritional supplements, drugs, and traditional medicines, and have a wide range of pharmacological actions. Rubiadin, a 1,3-dihydroxy-2-methyl anthraquinone, primarily originates from *Rubia cordifolia* Linn (Rubiaceae). It was first discovered in 1981 and has been reported for many biological activities. However, no review has been reported so far to create awareness about this molecule and its role in future drug discovery. Therefore, the present review aimed to provide comprehensive evidence of Rubiadin's phytochemistry, biosynthesis, physicochemical properties, biological properties and therapeutic potential. Relevant literature was gathered from numerous scientific databases including PubMed, ScienceDirect, Scopus and Google Scholar between 1981 and up-to-date. The distribution of Rubiadin in numerous medicinal plants, as well as its method of isolation, synthesis, characterisation, physicochemical properties and possible biosynthesis pathways, was extensively covered in this review. Following a rigorous screening and tabulating, a thorough description of Rubiadin's biological properties was gathered, which were based on scientific evidences. Rubiadin fits all five of Lipinski's rule for drug-likeness properties. Then, the in depth physicochemical characteristics of Rubiadin were investigated. The simple technique for Rubiadin's isolation from *R. cordifolia* and the procedure of synthesis was described. Rubiadin is also biosynthesized via the polyketide and chorismate/o-succinylbenzoic acid pathways. Rubiadin is a powerful molecule with anticancer, antiosteoporotic, hepatoprotective, neuroprotective, anti-inflammatory, antidiabetic, antioxidant, antibacterial, antimalarial, antifungal, and antiviral properties. The mechanism of action for the majority of the pharmacological actions reported, however, is unknown. In addition to this review, an in silico molecular docking study was performed against proteins with PDB IDs: 3AOX, 6OLX, 6OSP, and 6SDC to support the anticancer properties of Rubiadin. The toxicity profile, pharmacokinetics and possible structural modifications were also described. Rubiadin was also proven to have the highest binding affinity to the targeted proteins in an in silico study; thus, we believe it may be a potential anticancer molecule. In order to present Rubiadin as a novel candidate for future therapeutic development, advanced studies on preclinical, clinical trials, bioavailability, permeability and administration of safe doses are necessary.

**Keywords:** Rubiadin, *Rubia cordifolia*, biosynthesis, physicochemical properties, anticancer, pharmacology

## Graphical Abstract



## Introduction

The most important translational research endeavor that contributes to human health and well-being is drug discovery. All efforts involved in changing a drug-like molecule to a final licensed drug product for marketing by the necessary regulatory authorities are referred to as drug development. Identifying and screening of small molecules for their therapeutic benefits and biological properties are critical phases for drug discovery and development. Most of the well-known compounds in the world has been documented in a library that was created over a long period of time. Among those compounds or small molecules, most of them are derived from natural resources in the past. Currently, the researchers have access to a wide range of chemical substances and hundreds of thousands of novel compounds have also been discovered through high-throughput and combinatorial chemical processes. It remains to be identified which of these millions of molecules have the features that will allow them to become drugs.

Anthraquinones (AQs) are the biggest group of compounds with natural colors, with over 700 chemicals identified thus far. Plants provided approximately 200 of these chemicals, with

the remaining coming from lichens and fungus.<sup>1,2</sup> AQs are found in all plant parts including the roots, rhizomes, fruits and flowers with the majority produced from 9,10-anthracenedione. These compounds are also found in peas, cabbage, lettuce and beans.<sup>3</sup> Due to their wide range of applications, AQs and their derivatives are among the most extensively utilized phytochemicals in the food and pharmaceutical industries. Studies have shown that AQs have been their reported for antioxidant,<sup>4</sup> antitumor,<sup>5-9</sup> anti-inflammatory,<sup>9,10</sup> diuretic,<sup>9</sup> antiarthritic,<sup>11</sup> antifungal,<sup>12</sup> antibacterial,<sup>13</sup> and antimalarial<sup>14</sup> activities. AQ derivatives are a very useful category in the search for anticancer medicines. AQ-based drugs such as doxorubicin, valrubicin, mitoxantrone, idarubicin, and epirubicin have been used successfully to treat hematological and solid malignancies. Therefore, the AQs core continues to be a potential scaffold for developing novel therapeutic candidates.<sup>15</sup>

Rubiadin, a 1,3-dihydroxy-2-methyl anthraquinone (Figure 1), is primarily obtained from *Rubia cordifolia* Linn (*R. cordifolia*), which belongs to Rubiaceae family. It is an essential component in the Ayurvedic system of medicine in the treatment of various diseases.<sup>16</sup> Rubiadin, which is

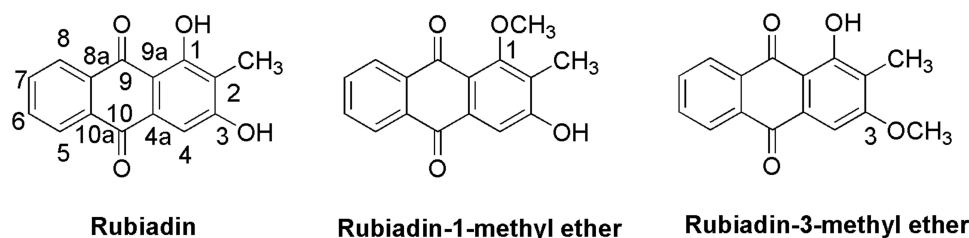


**Figure 1** Chemical structures of Rubiadin and its analogues.  
**Note:** Created with ChemDraw Ultra 8.0.

ubiquitous in many natural products, has sparked a lot of interest in recent years due to its excellent pharmacological effects including anticancer, antiosteoporotic, hepatoprotective, neuroprotective, anti-inflammatory, antidiabetic, antioxidant, antibacterial, antimalarial, antifungal, and antiviral activities. Nevertheless, despite its various therapeutic effects, it lacks a thorough and comprehensive review, to date. Hence, in the present review, the phytochemistry, biosynthesis and physicochemical properties of Rubiadin is summarized, with a particular focus on its biological activity. In order to strengthen this review, we have carried out molecular docking studies with selected proteins to prove its anticancer mechanism. It is hoped that the scientific evidence from this review can serve as a solid foundation for further research and provide important information for developing Rubiadin as a therapeutic agent and health product.

## Methods

Relevant literature was collected from PubMed, ScienceDirect, Scopus and Google Scholar. The following keywords were used in the search: “Rubiadin” OR 1,3-dihydroxy-2-methyl anthraquinone OR 9,10-anthracenedione AND “Chemistry” OR “Biosynthesis” OR “in-vitro” OR “in-vivo” OR “Biological studies” OR “Pharmacological studies” OR “Toxicity” OR “Pharmacokinetics” OR “Pharmacodynamics” OR “Pharmacokinetics” OR “Pharmacodynamics”. An initial screening was performed on studies that were not written in English or did not have any abstracts. The review’s data was divided into two main categories: Rubiadin’s chemical and biological properties. The scientific evidence gathered is summarized and incorporated following a thorough screening.

## Phytochemistry of Rubiadin

### Origin and Distribution

Rubiadin is primarily isolated from the root of *R. cordifolia*, a Rubiaceae family. *R. cordifolia* is an important

medicinal plant used in the Ayurvedic system of medicine in the treatment of a variety of diseases.<sup>16</sup> *Morinda officinalis* (*M. officinalis*) which is another major source of Rubiadin<sup>17</sup> is a commonly used traditional Chinese medicine which has been used in China for many years. Additionally, Rubiadin is also found in a traditional medicine named *Manjisthadi churna*, which consists of lesser cardamom, used in the treatment of hyperlipidemia in India’s Ayurvedic system of medicine and traditional medical practices.<sup>18</sup> It is also found in some traditional Chinese medicines including *Jia-Jian-Di-Huang-Yin-Zi* decoction which is a seven-herb component consisting of *Radix rehmanniae*, *Fructus corni*, *Radix morindae officinalis*, *Herba cistanches*, *Radix angelicae sinensis*, *Radix asparagi* and *Radix paeoniae alba*<sup>19</sup> as well as another decoction named *Er Xian*<sup>20</sup> which is a six-herb component consisting of *Herba epimedii*, *Radix morindae officinalis*, *Radix angelicae sinensis*, *Rhizoma anemarrhenae*, *Cortex phellodendri* and *Rhizoma curculiginis*. Medicinal plants containing Rubiadin, Rubiadin-1-methyl ether (RBME) and Rubiadin-3-methyl ether are summarized in Table 1.

### Medicinal Uses of *R. cordifolia*

*R. cordifolia*, also known as Indian madder or *Manjistha*, is a medicinal plant that grows in the forests of Pakistan, India, China, Korea, Japan and Mongolia.<sup>21</sup> Based on ethnobotanical reports, its roots are used in the treatment of jaundice while the stems are used to treat snake bites and scorpion stings. It is also useful against diabetic foot ulcers.<sup>22</sup> Traditionally, *R. cordifolia* is used for chronic pyrexia and puerperal fever, as well as a common medicine to alleviate heat and itching in eczema, psoriasis, herpes and scabies. When combined with honey, it is also deemed as effective against vitiligo.<sup>23</sup> Other therapeutic effects include as an immunomodulator, analgesic, diuretic, gastroprotective, hepatoprotective, antioxidant, wound healing, nephroprotective and antiviral properties.<sup>24–27</sup>

**Table 1** List of Medicinal Plants Containing Rubiadin

Plant Source	References
<b>Rubiadin</b>	
<i>Rubia cordifolia</i>	Dosseh et al <sup>82</sup> ; Tripathi et al <sup>28</sup> ; Tripathi and Sharma <sup>61</sup> ; Rao et al <sup>16</sup> ; Shen et al <sup>83</sup>
<i>Morinda officinalis</i>	Liu et al <sup>84</sup> ; Zhang et al <sup>85</sup> ; Zhao et al <sup>86</sup> ; Shi et al <sup>17</sup>
<i>Prismatomeris connata</i>	Peng et al <sup>30</sup>
<i>Heterophyllaea pustulata</i>	Montoya et al <sup>47</sup> ; Comini et al <sup>38</sup> ; Vittar et al <sup>39</sup> ; Marioni et al <sup>65</sup> ; Micheloud et al <sup>48</sup> ; Micheloud et al <sup>49</sup> ; Cogno et al <sup>37</sup> ; Mugas et al <sup>87</sup>
<i>Rubia tinctorum</i>	Schunck <sup>88</sup> ; Kawasaki et al <sup>89</sup> ; Cuoco et al <sup>90</sup> ; Cooksey <sup>91</sup>
<i>Prismatomeris malayana</i>	Tuntiwachwuttikul et al <sup>92</sup>
<i>Lilium leucanthum</i>	Khan et al <sup>64</sup>
<i>Hymenodictyon excelsum</i>	Rahman <sup>93</sup>
<i>Hedyotis capitellata</i>	Ahmad et al <sup>94</sup>
<i>Rubia peregrina</i>	Usai and Marchetti <sup>95</sup>
<i>Morinda umbellata</i>	Chiou et al <sup>40</sup>
<i>Prismatomeris fragrans</i>	Kanokmedhakul et al <sup>42</sup>
<i>Morinda citrifolia</i>	Bussmann et al <sup>96</sup>
<i>Morinda elliptica</i>	Ali et al <sup>41</sup>
<i>Prismatomeris sessiliflora</i>	Likhitwitayawuid et al <sup>68</sup>
<i>Ophiorrhiza shendurunii</i>	Rajan et al <sup>97</sup>
<i>Rennellia elliptica</i>	Osman et al <sup>98</sup>
<i>Knoxia valerianoides</i>	Yuan and Zhao <sup>99</sup> ; Yoo et al <sup>100</sup> ; Zhao et al <sup>101</sup>
<i>Blumea aromatica</i>	Lan et al <sup>102</sup>
<i>Prismatomeris tetrandra</i>	Jiang et al <sup>103</sup>
<i>Hedyotis diffusa</i>	Huang et al <sup>104</sup>
<i>Rhynchotechum vestitum</i>	Liu et al <sup>105</sup>
<i>Swietenia mahagoni</i>	Haque et al <sup>106</sup>
<b>Rubiadin-1-methyl ether</b>	
<i>Pentas schimperi</i>	Mohr et al <sup>56</sup>
<i>Morinda officinalis</i>	Li et al <sup>107</sup> ; He et al <sup>51</sup> ; Zhang et al <sup>85</sup>
<i>Morinda coreia</i>	Chokchaisiri et al <sup>108</sup>
<i>Heterophyllaea pustulata</i>	Comini et al <sup>70</sup> ; Cogno et al <sup>37</sup>
<i>Prismatomeris fragrans</i>	Kanokmedhakul et al <sup>42</sup>
<i>Prismatomeris sessiliflora</i>	Likhitwitayawuid et al <sup>68</sup>
<i>Rennellia elliptica</i>	Osman et al <sup>98</sup>
<i>Prismatomeris tetrandra</i>	Jiang et al <sup>103</sup>
<i>Knoxia valerianoides</i>	Zhao et al <sup>101</sup>
<i>Paederia scandense</i>	Zou et al <sup>109</sup>
<i>Rhynchotechum vestitum</i>	Liu et al <sup>105</sup>
<i>Xanthophytum atropvensis</i>	Li et al <sup>110</sup>
<i>Neonauclea calycina</i>	Tosa et al <sup>111</sup>
<b>Rubiadin-3-methyl ether</b>	
<i>Prismatomeris memecyloides</i>	Khanh et al <sup>112</sup>
<i>Craib</i>	
<i>Morinda angustifolia</i>	Chen et al <sup>113</sup>
<i>Uvaria kurzii</i>	Lv et al <sup>114</sup>

## Isolation of Rubiadin

The powdered root parts of *R. cordifolia* are extracted using a cold percolation in 50% aqueous ethanol following

by a drying step using a rotary evaporator under a reduced pressure and a controlled temperature. In a separating funnel, the solvent-free extract is portioned with a 90%

aqueous methanol and n-hexane. The n-hexane layer is removed and the aqueous-methanolic layer is subsequently dried and suspended in water for a further extraction step using chloroform (fraction 2) and n-butanol extractions in successive manner. Fraction 2 is chromatographed on a silica gel followed by an elution step with hexane, toluene, ethyl acetate and butanol (in order of increasing polarity) using varied solvent ratios. The column is further eluted with a toluene-hexane (1:1) combination, yielding a yellow solid. The solid is purified by numerous recrystallization processes using toluene and is further validated by a thin layer chromatography using toluene:ethyl acetate (85:15) as the mobile phase ( $R_f = 0.58$ ). The spots are finally observed under UV irradiation.<sup>16,28</sup>

## Synthesis of Rubiadin

In the first step, the condensation of phthalic anhydride (1) and 2,6-dihydroxytoluene (2) with  $\text{CH}_2\text{ClCH}_2\text{Cl}/\text{CHCl}_2\text{CHCl}_2$  in the presence of aluminium chloride yielded 2-(2',4'-dihydroxy-3'-methyl) benzoylbenzoic acid (3). Then, in the second step, cyclization via dehydration of the compound 3 is performed in the presence of fused boric acid with concentrated sulphuric acid at 100 °C for 25 min to yield Rubiadin<sup>29</sup> (Figure 2).

## Structural Characterization of Rubiadin

A very detailed structural characterization of Rubiadin is given below based on the values obtained from spectroscopic methods including ultraviolet (UV), Fourier-transformed infrared (FTIR),  $^1\text{H}$ -nuclear magnetic resonance (NMR),  $^{13}\text{C}$ -NMR and EI-MS.<sup>30</sup> The UV spectra of Rubiadin indicates a  $\lambda_{\text{max}}$  at 408 nm for  $n-\pi^*$  transition and at 279 and 251 for  $\pi-\pi^*$  transitions. The IR spectra shows absorption bands at 3396 (OH), 2923, (C-H), 1661 (C=O non-chelated) and at 1623, 1589 (C=C aromatic) representing the characteristic groups of Rubiadin. It also shows a molecular ion peak at  $m/z$  254.12 in EI-MS and analysed for a molecular formula  $\text{C}_{15}\text{H}_{10}\text{O}_4$ .

The  $^1\text{H}$ -NMR spectrum reveals the presence of a hydrogen-bonded hydroxyl group at  $\delta$  13.06 (1H, s] and another phenolic hydrogen at  $\delta$  11.22 (1H, br.s.). The strong singlet for three protons at  $\delta$  2.02 is due to the presence of a methyl group attached to the aromatic ring system while the singlet at  $\delta$  7.1 for one proton is due to an aromatic proton in H-4 position. On the other hand, the multiplet between  $\delta$  7.83 and 7.88 for two protons are attributed to aromatic protons at H-6 and H-7 positions. A pair of doublet of doublets at  $\delta$  8.08 (dd, 1H,  $J = 1.5, 7.5$  Hz) and 8.12 (dd, 1H,  $J = 1.5, 7.5$  Hz) are assigned to H-8 and H-5, respectively. In its  $^{13}\text{C}$ -NMR spectrum, there were 15 signals out of which two signals at  $\delta$  186.2 and 181.78 are due to conjugated carbonyl carbons and are characteristic signals of anthraquinoid nucleus. The signal present in the upfield region at  $\delta$  8.09 is due to the methyl carbon while the signal at  $\delta$  108.9 is assigned to C-2 carbon. The two phenolic carbons appeared at  $\delta$  162.82 and 162.46 where the carbon atoms adjacent to the phenolic carbons resonated at  $\delta$  107.35 (C-4) and 117.3 (C-9a). The remaining signals at  $\delta$  134.54 (C-8a), 134.44 (C-10a), 132.98 (C-4a), 132.87 (C-6), 131.70 (C-7), 126.70 (C-5) and 126.37 (C-8) are characteristic signals off the unsubstituted aromatic ring of the AQ system.<sup>30</sup>

## Physicochemical and Drug-Likeness Properties of Rubiadin

The physicochemical properties of Rubiadin are mainly obtained from PubChem<sup>31</sup> and other reliable databases such as DruLiTo. Certain physicochemical features allow a molecule to be converted into a drug-like molecule: 1) molecule should be small enough to be transported throughout the body, 2) hydrophilic enough to dissolve in the blood stream, 3) lipophilic enough to cross fat barriers within the body and 4) contain enough number of polar groups to bind to a receptor but not too many which leads elimination too quickly from the body via urine to exert the therapeutic effect (Table 2). The drug-like properties (molecular weight, H-bond donors, H-bond acceptors, log

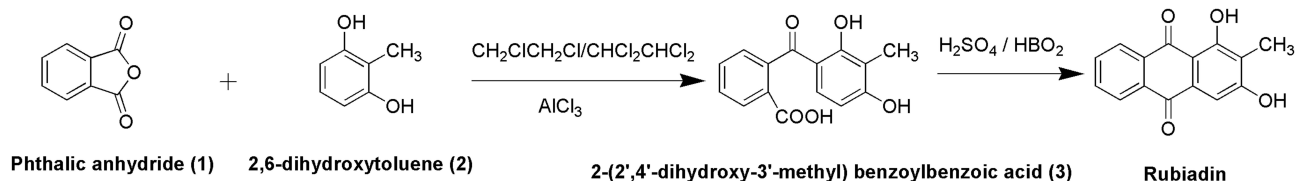


**Figure 2** Synthesis of Rubiadin.

**Note:** Created with ChemDraw Ultra 8.0.

**Table 2** Computed Physicochemical Properties of Rubiadin

Property	Value/Result
Common name	Rubiadin
Synonyms	1,3-Dihydroxy-2-methylantracene-9,10-dione; 9,10-anthracenedione-1,3-dihydroxy-2-methyl-Rubiadine
Category	Anthraquinone
IUPAC name	1,3-Dihydroxy-2-methylantracene-9,10-dione
Canonical SMILES	<chem>CC1=C(C=C2C(=C1O)C(=O)C3=CC=CC=C3C2=O)O</chem>
Molecular formula	C <sub>15</sub> H <sub>10</sub> O <sub>4</sub>
Molecular weight	254.06 g/mol
Hydrogen bond donors	2
Hydrogen bond acceptors	4
Rotatable bonds	0
Log P (partition coefficient value)	0.809 (Predicted)
Molar refractivity	68.83
Topological polar surface area	74.6 Å <sup>2</sup>
Percent composition	C: 0.709, H: 0.040, O: 0.252
XLogP3-AA	3.1
Molar mass	254.05790880 Da
Monoisotopic mass	254.05790880 Da
Heavy atom count	19
Formal charge	0
Complexity	405
Isotope atom count	0
Atom stereocenter count	0
Bond stereocenter count	0
Covalently bonded unit count	1
Canonicalized	1
Melting point	290 °C
Boiling point	527 °C
Appearance	Yellow needle shape
Solubility	Ethyl acetate
Density	1.5 g/mL
Pka	6.350
Molar volume	215.17
Molecular polar surface area	74.6 Å <sup>2</sup>
Molecular 3D-polar SASA	419.12
Molecular SASA	411.10
Molar refraction	72.28 cm <sup>3</sup> /mol

P value and rotatable bonds) as described in Lipinski's rule of five<sup>32</sup> are calculated using Biovia Discovery studio 19.0. Any drug-like compound should have 1) a molecular weight of 500, 2) a partition coefficient (log P)-value of 5, 3) H-bond donors of 5, 4) H-bond acceptors of 10 and 5) rotatable bonds of 10 according to Lipinski's rule of five. Since compounds that do not break Lipinski's rule of five may have improved folding, polarity and molecular size, the drug-like molecules are assumed to have the predicted therapeutic benefits.<sup>33</sup> The objective of the suggested method is to deliver primary evidence defining the

potential physical properties of the compounds, rather than serving as a rigid screening criteria in itself, since Lipinski's rule of five is an effective and valid guide for forecasting the potential for oral exposure to enhanced chemical compounds. Overall, Rubiadin appears to match all five of Lipinski's drug-likeness criteria (Table 2). According to the data acquired from DruLiTo software, Rubiadin also passed the Ghose filter, Veber's rule, blood-brain barrier (BBB) likeness rule, Unweighted Quantitative Estimate of Drug-likeness (QED), and Weighted QED, but failed the CMC-50 like rule and

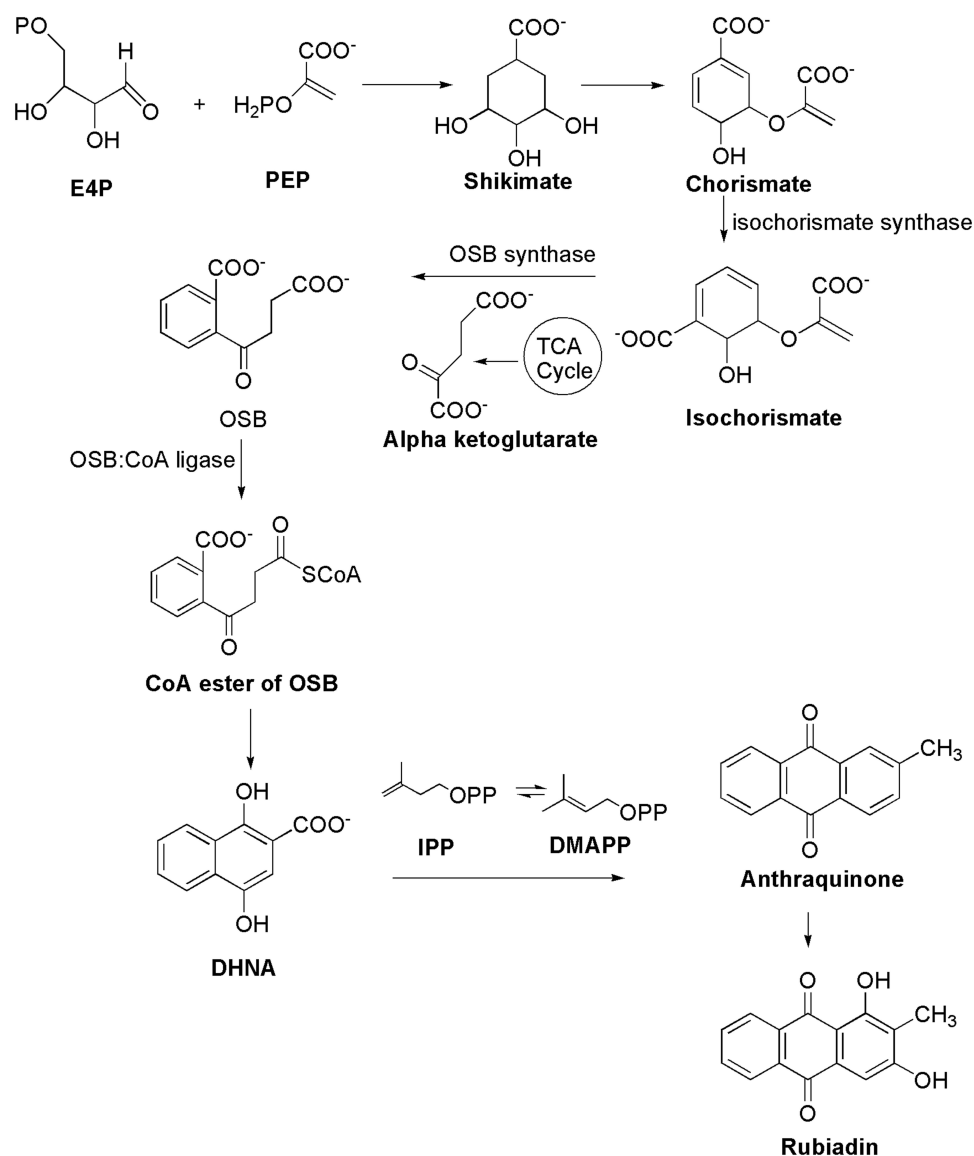


**Figure 3** Biosynthesis of Rubiadin.

**Note:** Created with ChemDraw Ultra 8.0.

MDDR like rule. All of the above findings indicate that it is a good potential therapeutic agent for a variety of disorders.

## Biosynthesis of Rubiadin

AQs are derived from a variety of precursors and pathways in nature. Two biosynthesis pathways have been established: 1) the polyketide and 2) the chorismate/*o*-succinylbenzoic acid pathways, despite the fact that their biosynthetic processes remain unknown. Rubiadin is made by combining phosphophenol pyruvate (PEP) with erythrose-4-phosphate (E4P) to produce chorismate and isochorismate, which are then transformed to

*o*-succinylbenzoate (OSB) in the presence of  $\alpha$ -ketoglutarate (Figure 3). Rings A and B of Rubiadin are formed through the synthesis of 1,4-dihydroxy-2-naphthoic acid (DHNA) by a ring closure of OSB–CoA. Prenylation of the DHNA results in naphthoquinol or naphthoquinone, which is involved in the synthesis of ring C. Isopentenyl pyrophosphate (IPP), which can be generated from mevalonate (MVA) or 2-C-methyl-D-erythritol 4-phosphate (MEP), is required for the biosynthesis of AQs, including Rubiadin (Figure 4). In the late stages of biosynthesis, most AQs in the Rubiaceae undergo different alterations owing to hydroxylation or methylation, in which groups like as hydroxy and methyl groups are added to Rubiadin's ring C.<sup>34</sup>

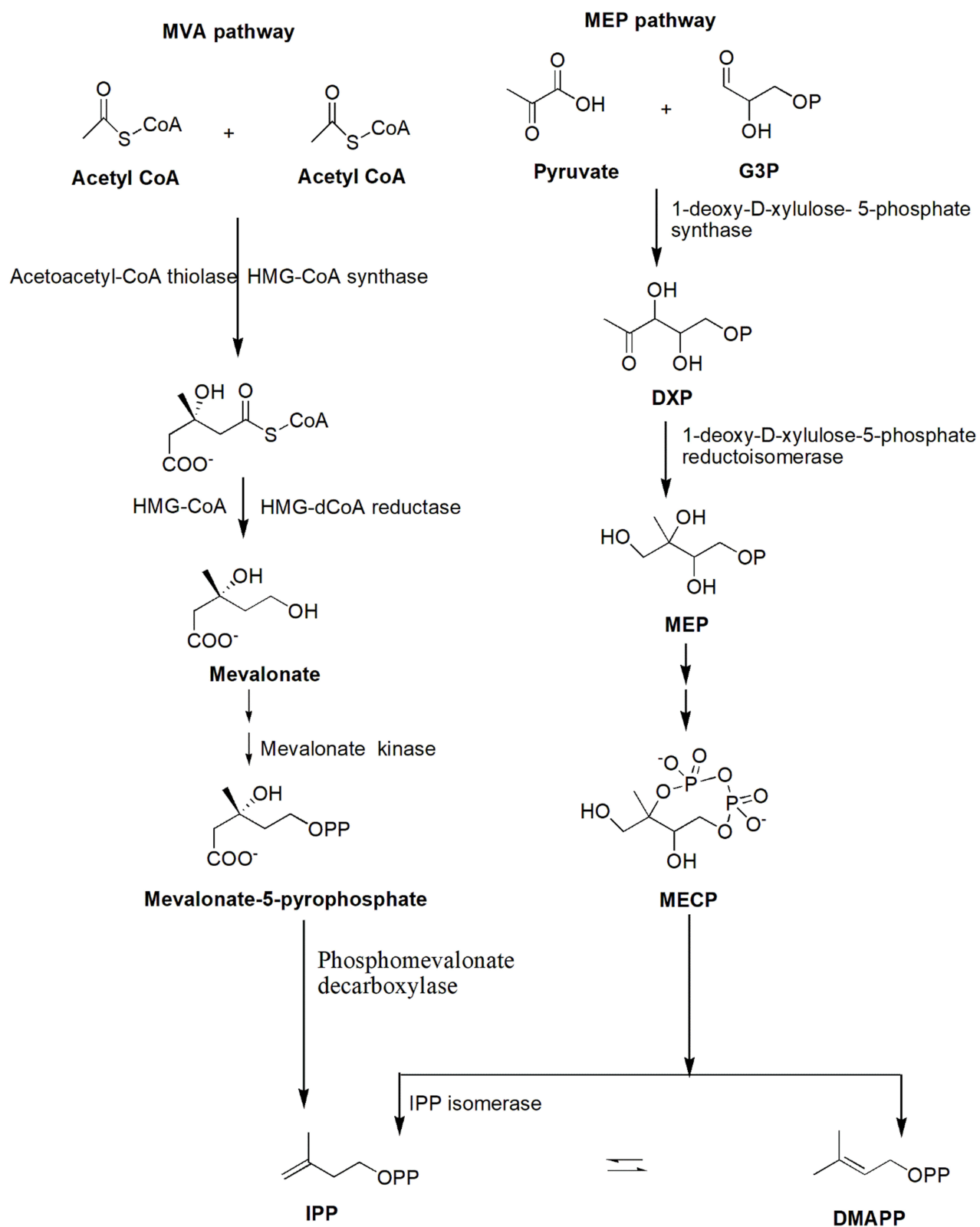


**Figure 4** MVA and MEP pathways for the synthesis of IPP.  
**Note:** Created with ChemDraw Ultra 8.0.



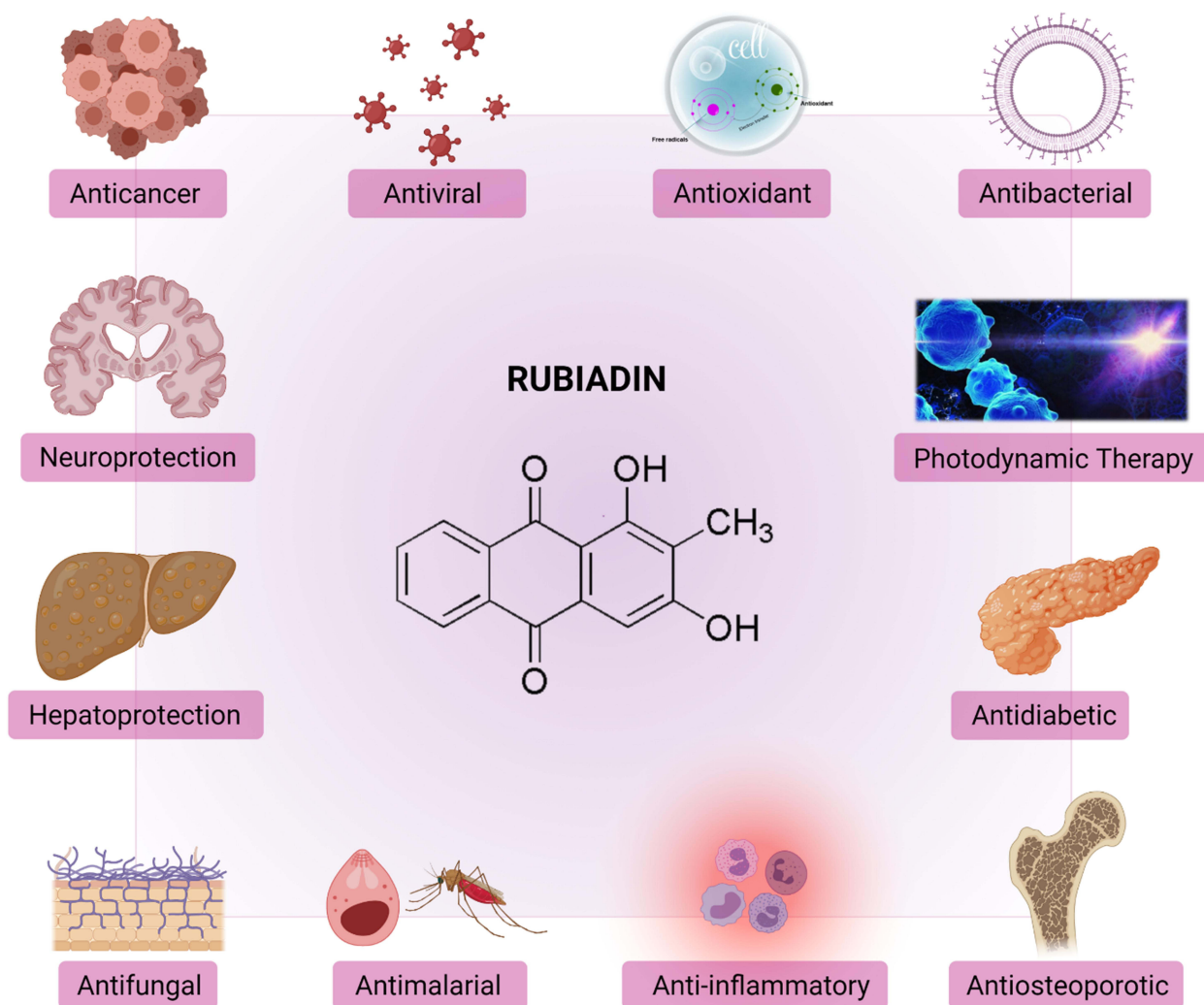


**Figure 5** Biological properties and therapeutic potential of Rubiadin.

**Note:** Created with BioRender.com.

## Biological Activities of Rubiadin

Rubiadin has been reported to possess many biological activities (Figure 5) as summarized below.

### Toxicity Profile

One of the latest acute toxicity study reported that oral administration of Rubiadin (100, 200, 500 and 1000 mg/kg) to Swiss albino mice using staircase/up and down method showed no significant toxicity.<sup>35</sup> Furthermore, mice given an aqueous extract of *R. cordifolia* and *R. tinctorum* (Rubiadin as one of the principal constituents) for 14 days indicated that the highest acceptable doses were 3500 mg/kg and 5000 mg/kg, respectively. In another study, both sexes of mice were administered with *R. cordifolia* root extract mixed in their diet (0–5%) for 90 days with no clinical signs of toxicity seen, although there were

some changes in kidney and epidermal vaginal cyst in some animals based on histological analysis. Overall, the findings indicate that Rubiadin is safe at the investigated dose levels (Figure 6).

### Anticancer Activity and Photodynamic Therapy

AQs have long been believed to have anticancer properties, acting primarily through DNA damage, cycle arrest and apoptosis.<sup>36</sup> Very recently, Cogno et al<sup>37</sup> evaluated the photoactivity of Rubiadin on monolayers and multicellular tumor spheroids following a photodynamic therapy. Rubiadin showed photosensitizing ability on monoculture of colon cancer cells (SW 480) at low concentration where necrosis has occurred. In addition, Comini et al<sup>38</sup>

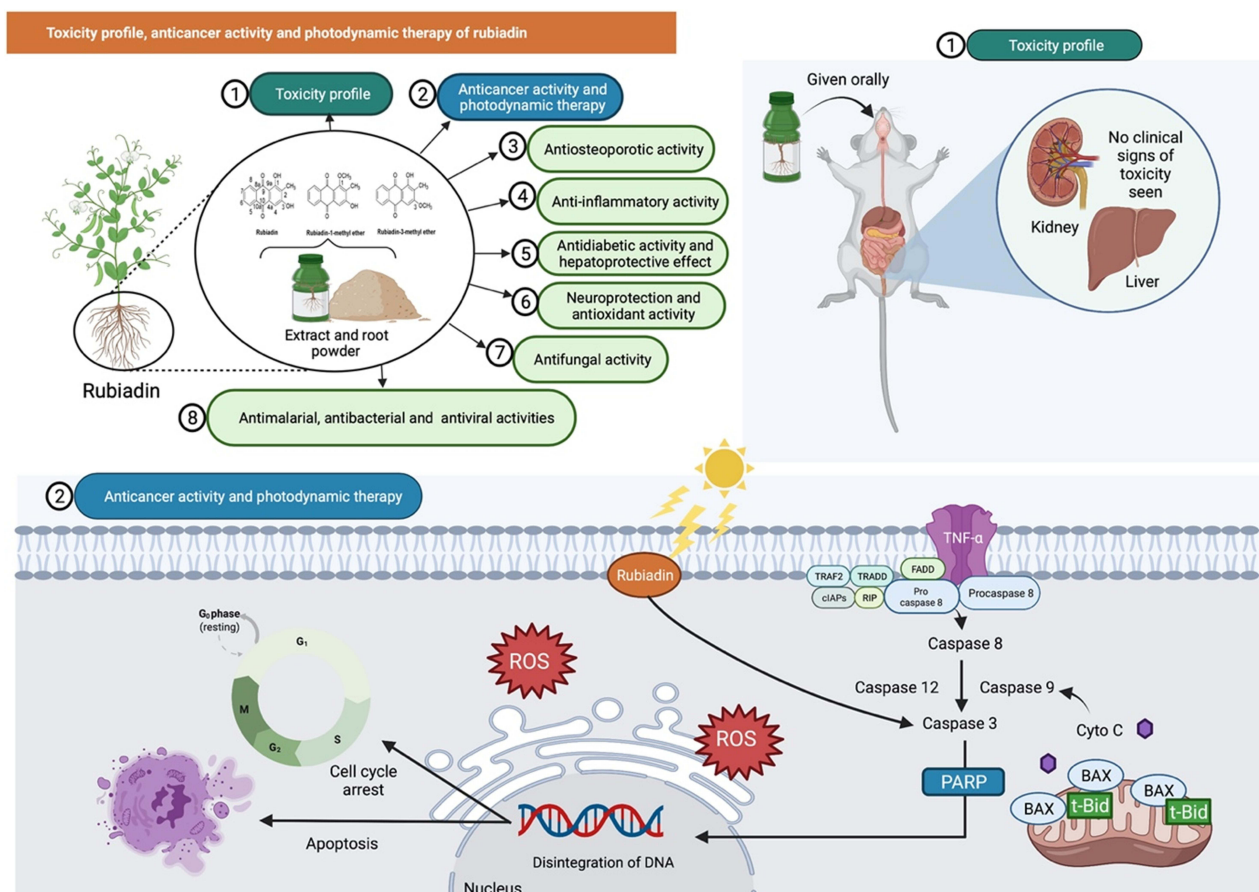


**Figure 6** Rubiadin's toxicity profile, anticancer activity, and photodynamic therapy. In the toxicity study, oral administration of rubiadin showed no clinical signs of toxicity seen indicating that the biochemical compound is safe at certain investigated dose levels. Through favorable photosensitizing ability of rubiadin, it can act as an anticancer by acting primarily through DNA damage, cycle arrest and apoptosis and be used in photodynamic therapy.

**Note:** Created with BioRender.com.

**Abbreviations:** TNF- $\alpha$ , tumor necrosis factor alpha; TRAF2, TNF receptor-associated factor 2; cIAPs, cellular inhibitors of apoptosis; TRADD, TNFR1-associated death domain protein; FADD, Fas-associated death domain protein; RIP, ribosome-inactivating protein; Bax, BCL2 associated X, apoptosis regulator; t-Bid, truncated Bid; Cyto C, cytochrome complex; PARP, poly (ADP-ribose) polymerase; ROS, reactive oxygen species.

investigated the potential role of Rubiadin and RBME as phototoxic agents against human breast cancer using MCF-7c3 cells. At 100  $\mu\text{M}$  and a light exposure of 1 J/cm<sup>2</sup>, both Rubiadin and RBME showed considerable photocytotoxicity on cancer cells. The observed cellular death by the photoactivated Rubiadin and RBME were closely related to a singlet oxygen production, with decreased cell viability in relation to tumor cell uptake. Subsequently, another study by Vittar et al<sup>39</sup> revealed that Rubiadin exhibited significant photocytotoxicity on human cancer cells (MCF-7c3) in a concentration-dependent manner. Additionally, biochemical analysis revealed the involvement of caspase-3, PARP cleavage and DNA fragmentation in Rubiadin-induced apoptosis (Figure 6).

In addition to the above studies, Rubiadin also exhibited significant cytotoxicity against HepG2 cells, with minimum

inhibitory concentration (IC<sub>50</sub>) values of 3.6, 4.4 and 4.8  $\mu\text{M}$ , respectively.<sup>40</sup> It also conferred cytotoxicity towards the CEM-SS (T-lymphoblastic leukaemia), MCF-7 (breast carcinoma) and HeLa (cervical carcinoma) cell lines with IC<sub>50</sub> of 3, 10 and >30  $\mu\text{g/mL}$ , respectively.<sup>41</sup> In another study, Rubiadin and RBME exhibited significant cytotoxicity against NCI-H187 cells, with IC<sub>50</sub> values of 14.2 and 4.5  $\mu\text{g/mL}$ , respectively,<sup>42</sup> indicating its potential anticancer effects.

However, madder color, a food coloring made from *Rubia tinctorum* roots, has been shown to cause cancer in rats' kidneys and liver. In F344 rats, treatment with Rubiadin (0.04%) for 23 weeks enhanced atypical renal tubules/hyperplasias and induced renal cell adenomas and carcinomas. Additionally, Rubiadin enhanced glutathione S-transferase placental form-positive liver cell foci and

major intestinal dysplasias thus suggesting that Rubiadin enhances renal preneoplastic lesions, with a weaker effect on dysplasia. Additionally, Rubiadin may also target the liver and large intestine, implying that it plays a significant role in madder color-induced carcinogenicity.<sup>43</sup> Based on another study by the same researcher, Rubiadin is a potent carcinogenic metabolite of madder color, targeting proximal tubule cells in the outer medulla,<sup>44</sup> although oxidative stress increased by lucidin-3-O-primeveroside or alizarin may also be involved in renal carcinogenesis by madder color.

From another study, the excretion of lucidin and rubiadin was observed in rats following administration of lucidinprimeveroside (Lup). Lup was reduced to Rubiadin primeveroside which in turn, was hydrolyzed to Rubiadin, when treated with rat liver extract and nicotinamide adenine dinucleotide phosphate (NADPH). Rubiadin was more potent than lucidin but has similar effect to the positive control 7,12-di-methylbenz[ $\alpha$ ]anthracene in the unscheduled DNA synthesis experiment in primary rat hepatocytes. The uptake of the AQs glycosides alizarinprimeveroside (Alp) and Lup results in the production of a rodent carcinogen 1-hydroxyanthraquinone, as well as the highly genotoxic compounds lucidin and Rubiadin.<sup>45</sup>

The latest scientific evidence has demonstrated that novel AQs can inhibit cancer by paraptosis, autophagy, radiosensitization, thus overcoming chemoresistance.<sup>36</sup> However, scientists are still far from having a full understanding on the anticancer properties of Rubiadin, since some report mentioned it is also carcinogenic.<sup>43,44</sup> Thus, more in vivo and preclinical research are needed to fully understand its apparent potential in preventing and treating a variety of malignancies.

Although photoactivity is known for decades, only recently that it resurfaced as a potential therapy option for cancer and microbial diseases. Its key innovative component is light as the external factor since light can activate drugs locally, besides having a high level of selectivity and conferring minimal side effects.<sup>46</sup> Animals that ingest the aerial parts of *H. pustulata* show a classic primary photosensitization reaction, which is clinically characterized as dermatitis and, in severe cases, blindness. *H. pustulata* grows mainly in the Andes region of northwest Argentina. Rubiadin, a major compound in *H. pustulata*, is characterized as either a Type I or II photosensitizer, depending on its physicochemical features. Oral administration of Rubiadin can reproduce natural in experimental animals.

The presence of Rubiadins in the serum was identified and quantified in the skin of experimental animals using high performance liquid chromatography.<sup>47</sup> Since *H. pustulata* contains photosensitizing AQs such as Rubiadin and soranjidiol, the plant can cause dermal lesions through photosensitization.<sup>48</sup> Another study reported that Rubiadin and soranjidiol should be administered between 24 and 72 hours after *H. pustulata* ingestion, in order to coincide with the time when clinical indications are more noticeable. The clinical findings were validated for the presence of Rubiadin and soranjidiol in sera, although Rubiadin and soranjidiol were absent in skin samples. Finally, toxicological investigations on both compounds are important, since several recent researches have suggested that they could be used in photodynamic therapy.<sup>49</sup>

Rubiadin confer a favorable response to photodynamic therapy and therefore should be further examined. Additionally, any interaction between its use in reversing drug-resistant phenotypes and its photosensitizing effect should be further investigated.

## Antiosteoporotic Activity

Low bone mineral density (BMD) and micro-architectural deterioration of bone tissue are characteristic of osteoporosis, resulting in increased bone fragility and fracture risk.<sup>50</sup> He et al<sup>51</sup> investigated the in vitro effect of RBME on osteoclasts and the underlying mechanism. RBME inhibited the expression of osteoclast-related proteins such as nuclear factor of activated T-cells cytoplasmic 1 (NFATc1), cellular oncogene Fos (c-Fos), matrix metalloproteinase 9 (MMP-9) and cathepsin K (CtsK), as determined by Western blot analyses. RBM also reduced the nuclear translocation of p65 and inhibited the phosphorylation of nuclear factor kappa B (NF- $\kappa$ B) p65 and the degradation of nuclear factor of kappa light polypeptide gene enhancer in B-cells inhibitor alpha (I $\kappa$ B $\alpha$ ) indicating that RBME may be a promising agent for the prevention and treatment of bone disorders characterized by excessive bone resorption, due to its ability to inhibit osteoclastic bone resorption by blocking the NF- $\kappa$ B pathway (Figure 7).

Bao et al<sup>52</sup> investigated the in vitro effects of Rubiadin on bone resorption activity and its mechanism on osteoclasts derived from rat bone marrow cells. In a co-culture system of osteoblasts and bone marrow cells, Rubiadin reduced the formation of bone resorption pits, the number of multinucleated osteoclasts and the activity of tartrate resistant acid phosphates (TRAP) and cathepsin K. Additionally, Rubiadin increased the death of osteoclasts caused by macrophage colony stimulation factor (M-CSF) and receptor activator of

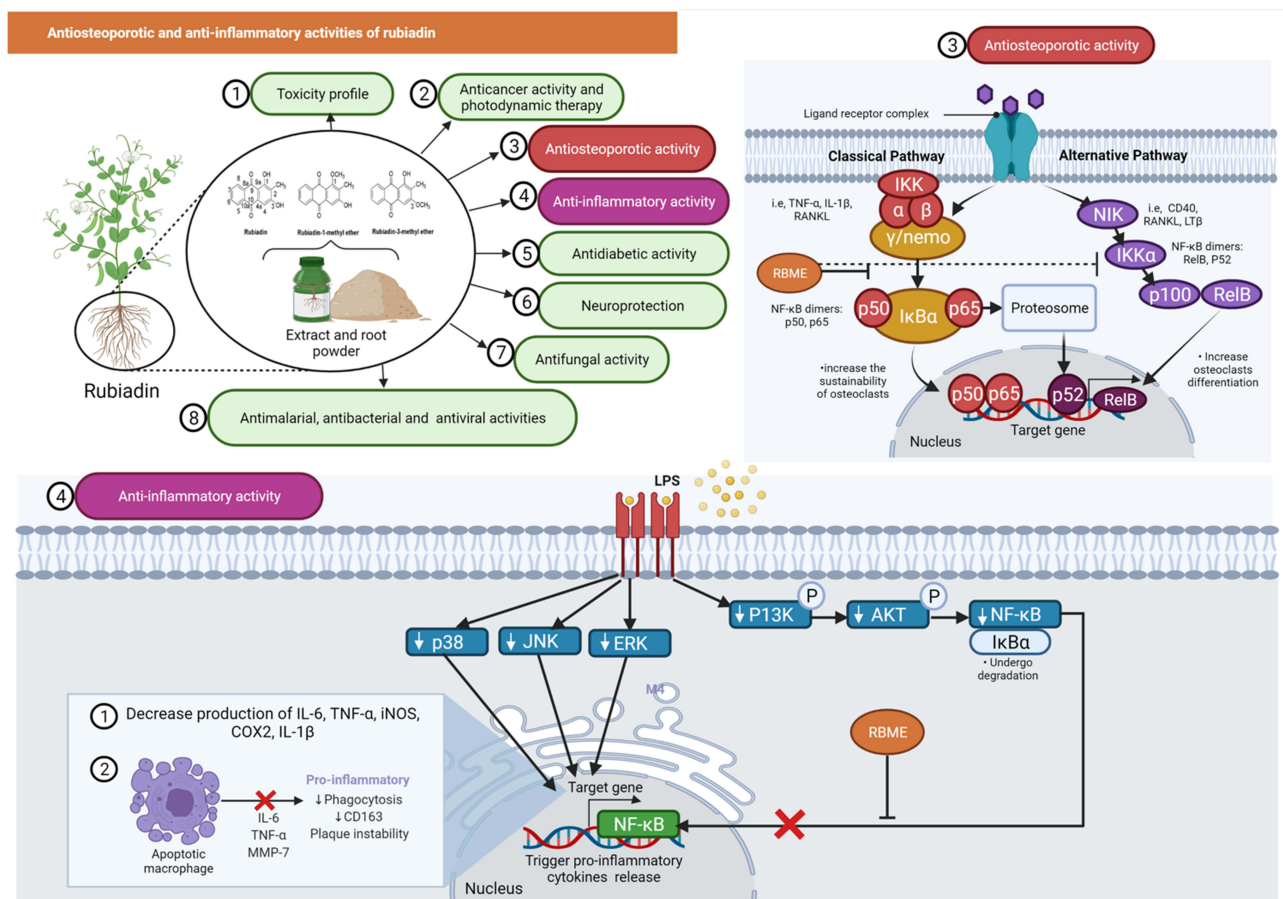


**Figure 7** Antiosteoporotic and anti-inflammatory activities of rubiadin. Inhibition of nuclear factor kappa B (NF-κB) phosphorylation and degradation of nuclear factor of kappa light polypeptide gene enhancer in B-cells inhibitor alpha (IκBα) by RBME suggests that it could be used to treat bone disorders characterized by excessive bone resorption. RBME demonstrated anti-inflammatory activity by decreasing pro-inflammatory markers while increasing the apoptotic rate of macrophages.

**Note:** Created with BioRender.com.

**Abbreviations:** TNF-α, tumor necrosis factor alpha; IL-1β and 6, interleukin 1 beta and 6; RANKL, receptor activator of nuclear factor kappa-B ligand; IKKγ/NEMO, nuclear factor-kappa B essential modulator; IκBα, nuclear factor of kappa light polypeptide gene enhancer in B-cells inhibitor, alpha; IKKα, inhibitory kappa B kinase α; NF-κB, nuclear factor kappa-light-chain-enhancer of activated B cells; NIK, NF-κB inducing kinase; CD40 & 163, cluster of differentiation 40 and 163; LTβ, lymphotoxin beta; RelB, RELB proto-oncogene, NF-KB subunit; ERK, extracellular signal-regulated kinase; JNK, c-Jun N-terminal kinase; P13K, phosphoinositide 3-kinases; AKT, protein kinase B/ AKT; iNOS, inducible nitric oxide synthase; COX2, cyclooxygenase-2; MMP-7, matrix metalloproteinase-7.

NF-κB ligand in bone marrow cells (RANKL). Rubiadin also 1) increased the ratio of osteoprotegerin (OPG), RANKL mRNA and protein expression in osteoblasts; 2) interfered the c-Jun N-terminal kinase (JNK) and NF-κB signaling pathways; and 3) reduced the expression of calcitonin receptor and carbonic anhydrase/II in osteoclasts induced from bone marrow cells with M-CSF and RANKL in osteoclasts. Overall, the findings suggest that Rubiadin may be a potential inhibitor for bone resorption.<sup>52</sup> Since RBME can inhibit osteoclast TRAP activity and bone resorption, it may be useful against osteoporosis.<sup>53</sup>

Xia et al<sup>54</sup> investigated the protective effect of *M. officinalis* on glucocorticoid-induced osteoporosis (GIOP)-modelled rats and osteoblasts. Eight weeks after dexamethasone (DEX) injection and *M. officinalis*

treatment in female rats aged 12 weeks, the BMD, micro-architecture of the trabecular bone, serum level of bone metabolism markers and urine metabolomics were assayed in vivo. The cultured osteoblasts were injured with DEX before the effects of *M. officinalis*, RBME on osteoblastic proliferation, differentiation and mineralization were investigated in vitro. *M. officinalis* increased BMD, improved the micro-architecture and intervened with bone metabolism via regulating alkaline phosphatase (ALP), tartrate resistant acid phosphatase (TRAP) and c-terminal telopeptides of type I collagen (CTX-I) levels. The in vitro experiment showed that *M. officinalis* and RBME increased the cell proliferation, ALP activity and enhanced extracellular matrix mineralization in DEX-injured osteoblasts.<sup>54</sup> Additionally, another study

demonstrated that multiple ingredients in a traditional Chinese medicine decoction named *Er-Xian* that included Rubiadin has anti-osteoporotic activity.<sup>20</sup> Although the data indicated that Rubiadin has action against bone tissue, more efficient and reliable bioassays should be urgently developed for thorough investigation of its antiosteoporotic mechanism before human clinical trials.

### Anti-Inflammatory Activity

Inflammation is a set of activities that occur in response to tissue damage associated with oxidative stress or other factors that initiate repair processes including as extracellular matrix remodeling and fibrosis.<sup>55</sup> Mohr et al<sup>56</sup> investigated the anti-inflammatory efficacy of RBME using an in vitro model of RAW 264.7 macrophages induced by lipopolysaccharide (LPS). The results indicated that RBME decreased the levels of pro-inflammatory markers such as nitric oxide (NOx), interleukin (IL)-6 and IL-1 with increased in macrophage apoptotic rate seen (Figure 7). The anti-inflammatory effects of Rubiadin-1-methyl ether was also investigated using an in vivo acute lung injury (ALI) induced by LPS (5 mg/kg, P.O.) by a similar group of researchers. Administration of RBME (3, 10 and 30 mg/kg, P.O.) decreased leukocyte infiltration, fluid leakage, NOx, IL-6, IL-12p70, interferon gamma (IFN- $\gamma$ ), tumour necrosis factor  $\alpha$  (TNF- $\alpha$ ) and monocyte chemoattractant protein-1 (MCP-1) levels as well as MPO activity (Mohr et al, 2019). RBME also enhanced the levels of IL-10 in the bronchoalveolar lavage fluid (BALF). On the other hand, Rubiadin's anti-inflammatory activity and potential mechanism of action, has yet to be confirmed and requires further research.

### Antidiabetic Activity

Mujeeb et al<sup>57</sup> evaluated the effectiveness of Rubiadin-loaded niosomes (RLN) in treating diabetic nephropathy (DN) that is induced by streptozotocin-nicotinamide (STZ-NA) in Wistar rats. In STZ-NA-induced DN rats, oral administration of RLN (100 and 200 mg/kg/week) markedly reduced blood glucose levels. Furthermore, RLN formulation significantly reduced urea, uric acid and creatinine levels while improving lipid, thiobarbituric acid reactive substances (TBARS), glutathione (GSH), superoxide dismutase (SOD) and catalase (CAT) levels in DN rats (Figure 8).<sup>57</sup> Nevertheless, other than this study, no other evidence of Rubiadin's anti-diabetic effectiveness has been found indicating that further studies are required to confirm Rubiadin's anti-diabetic properties.

### Hepatoprotective Activity

The hepatoprotective effect of Rubiadin was tested against carbon tetrachloride (CCl<sub>4</sub>)-induced liver injury in rats.<sup>16</sup> In CCl<sub>4</sub>-induced rats (1 mL/kg, i.p), the co-treatment of Rubiadin (50, 100 and 200 mg/kg, P.O.) for 2 weeks restored serum glutamic oxaloacetic transaminase, glutamate pyruvate transaminase, alkaline phosphatase (ALP),  $\gamma$ -glutamyltransferase ( $\gamma$ -GT), glutathione S-transferase and glutathione reductase levels to normal. Rubiadin also inhibited the development of hepatic malondialdehyde and the depletion of reduced glutathione level in the liver of CCl<sub>4</sub>-intoxicated rats in a dose-dependent manner, thus strongly suggesting that Rubiadin has a hepatoprotective effect against CCl<sub>4</sub>-induced hepatic damage in rats (Figure 8).<sup>16</sup> However, more research is needed in future to confirm Rubiadin's hepatoprotective potential especially in models that greatly mimic humans liver disease.

### Neuroprotection

The significant reduction in the onset of jerks and Straub tail along with a significant increase in onset of clonus and extensor were observed with pre-treatment of Rubiadin suspension (100 and 250 mg/kg, P.O.) for 3 days to the pentylene tetrazole (PTZ)-induced (80 mg/kg, i.p.) clonic-tonic convulsions in mice. Pre-treatment of Rubiadin suspension also significantly reduced the hind limb extension in maximal electro shock (MES)-induced seizures induced by delivering an electroshock at 50 mA using an electroconvulsometer through a pair of ear clip electrodes in Swiss albino mice. Rubiadin suspension (250 mg/kg) conferred some anticonvulsant effects in both MES- and PTZ-induced epileptic seizure models<sup>35</sup> overall indicating that Rubiadin is a potential neuroprotectant (Figure 8). The above study is a novel platform for testing Rubiadin against neurodegenerative disorders including Alzheimer's, Parkinson's and Huntington's disease.

### Antioxidant Activity

The antioxidant effects of AOs including Rubiadin are well known.<sup>58-60</sup> Rubiadin inhibits lipid peroxidation as induced by ferrous sulphate and *t*-butylhydroperoxide especially in Fe<sup>2+</sup>-induced lipid peroxidation (Figure 8). Rubiadin's antioxidant properties were comparatively higher than ethylenediaminetetraacetic acid (EDTA), tris, mannitol, vitamin E and *p*-benzoquinone.<sup>28</sup> Based on a follow-up study by Tripathi and Sharma,<sup>61</sup> Rubiadin inhibits lipid peroxidation in a dose-dependent manner. Apart

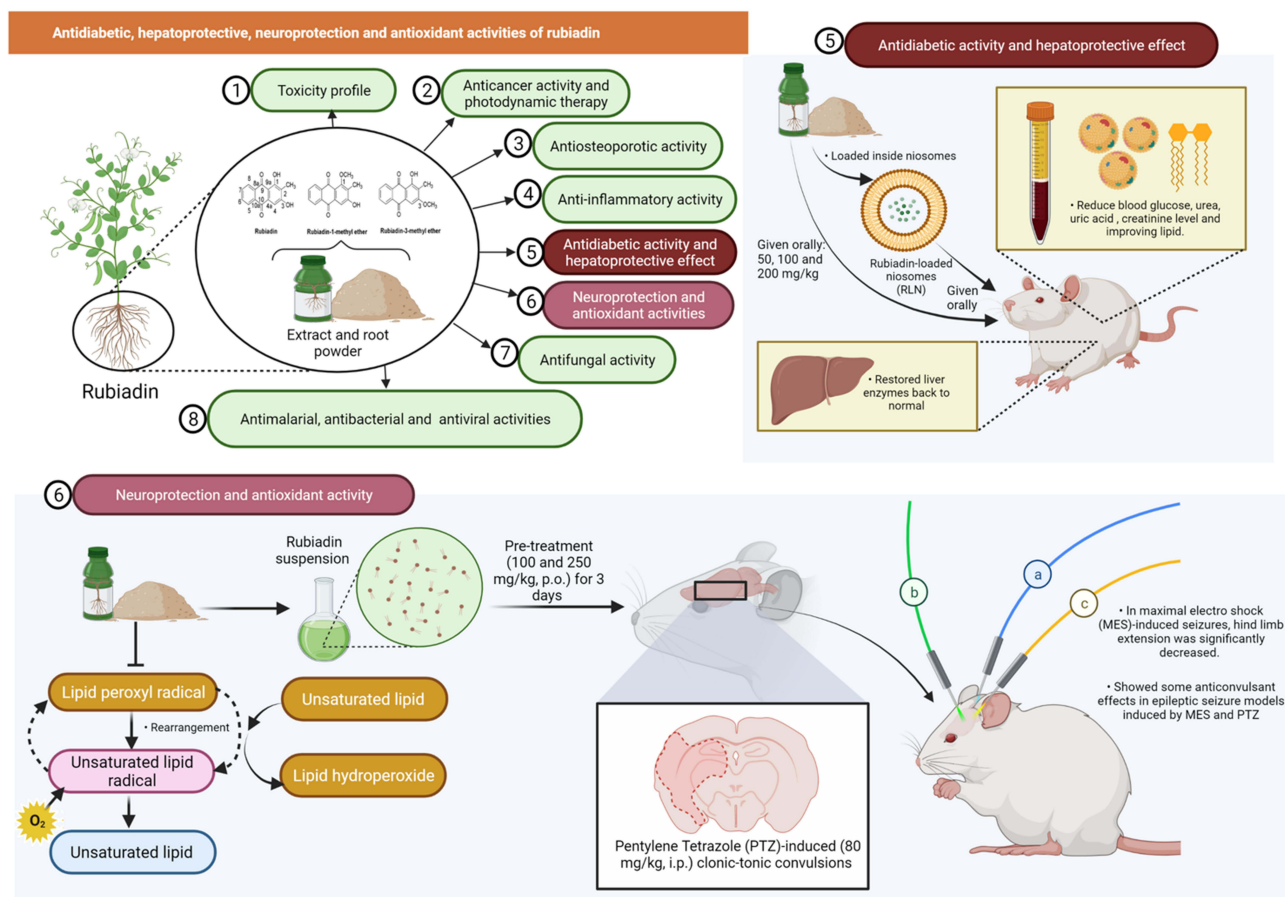


**Figure 8** Rubiadin's efficacy as an anti-diabetic, hepatoprotective, neuroprotective, and antioxidant. Rubiadin significantly decreased blood glucose and other serum biomarkers associated with the kidney and liver when taken orally, allowing them to return to normal levels. Rubiadin has also been identified as a potential neuroprotective and antioxidant compound, as it inhibits lipid peroxidation in dose-dependent manner in mice suffering from maximal electroshock (MES)-induced seizures.

**Note:** Created with BioRender.com.

from the studies mentioned above, no in vitro or in vivo antioxidant investigations on Rubiadin have been reported making relating the findings reported in a few models to antioxidant potential a challenge. Further research using a variety of approaches, including animal models with established mechanisms of action, should be conducted in the future to confirm Rubiadin's antioxidant potential.

### Antifungal Activity

AQs and their derived compounds are well documented for their antifungal properties.<sup>62,63</sup> *Bacillus velezensis* is a plant-growth-promoting rhizobacterium with enormous potential for agricultural development. *Bacillus velezensis* *Lle-9* which is isolated from *Lilium leucanthum* bulbs has shown antifungal activities against plant pathogens such as *Botryosphaeria dothidea*, *Fusarium oxysporum*, *Botrytis cinerea* and *Fusarium fujikuroi*. The presence of Rubiadin and other antimicrobial compounds in the bacterial culture can assist in isolating *Bacillus velezensis* *Lle-9*'s antifungal activity.<sup>64</sup>

Marioni et al<sup>65</sup> who investigated the antifungal effects of Rubiadin and RBME on *Candida tropicalis* confirmed that both compounds reduced biofilm formation and had an antifungal effect as mediated by oxidative and nitrosative stress under irradiation, with a significant increase in endogenous ROS and superoxide dismutase (SOD) activity. Rubiadin, in particular, altered the pro-oxidant-antioxidant balance. The most prominent effect of irradiation was oxidative stress, which altered the pro-oxidant-antioxidant balance and may contribute to an irreversible cell injury in the biofilm. Rubiadin is also an excellent synergistic combination with Amphotericin B indicating that the photosensitizing Rubiadin is a promising therapy option for *Candida* infections.<sup>65</sup> A follow-up study suggested that the  $O_2^{\cdot-}$  formed by an electron transfer quenches the Rubiadin and RBME excited states and is the main photosensitizing mechanism involved in the photo-induced antibiofilm activity.<sup>66</sup> Additionally, RBME behaves exclusively as a photosensitizer.<sup>67</sup>

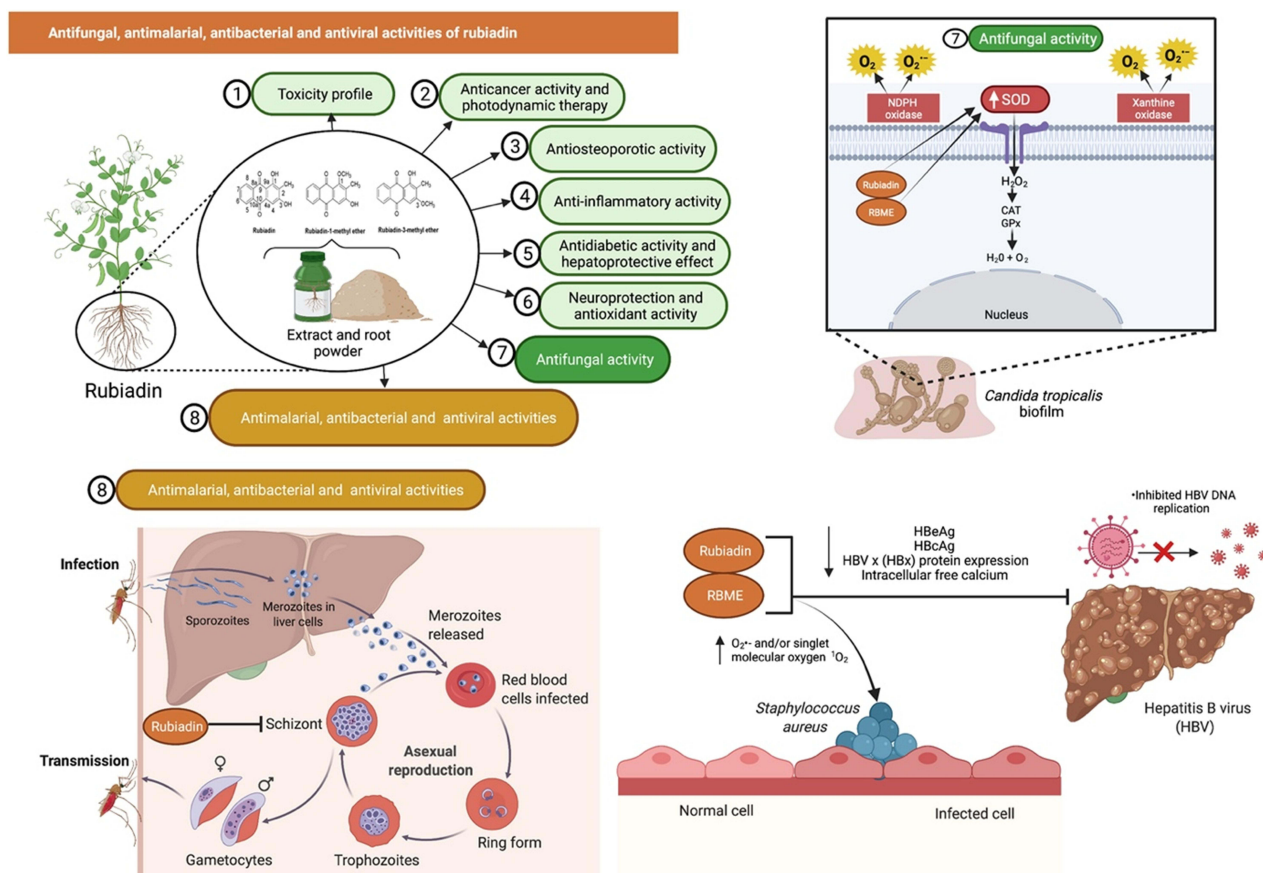


**Figure 9** Rubiadin's antifungal activity against *Candida tropicalis* confirmed that the compound inhibited biofilm formation and exerted antifungal activity with a significant increase in endogenous ROS and SOD activity. Additionally, rubiadin and RBME showed antimalarial and antibacterial properties, as the number of *Plasmodium falciparum* parasites (schizonts) and *Staphylococcus aureus* were significantly decreased. Rubiadin was tested against hepatitis B virus (HBV), and the results indicated that it inhibited HBV DNA replication, decreased hepatitis B e antigen (HBeAg) and hepatitis B core antigen (HBcAg) levels, HBV x (HBx) protein expression, and intracellular free calcium.

**Note:** Created with BioRender.com.

**Abbreviations:** ROS, reactive oxygen species; SOD, superoxide dismutase;  $H_2O_2$ , hydrogen peroxide; CAT, catalase; GPx, glutathione peroxidase;  $H_2O$ , water;  $O_2$ , oxygen;  $O_2^-$ , superoxide anion radical;  $^1O_2$ , singlet molecular oxygen.

The antifungal activity of Rubiadin has been evaluated against three fungi such as *Aspergillus ochraceus*, *Aspergillus niger* and *Candida lipolytica* where it showed moderate antifungal activity against *Aspergillus ochraceus* [minimum inhibitory concentration (MIC) of  $>80 \mu\text{g}/\text{disc}$ ] (Figure 9).<sup>41</sup> Overall, the findings suggest that Rubiadin and RBME have antifungal activity against a variety of pathogenic *Aspergillus* and *Candida* species. Rubiadin has the potential to be employed as a lead compound in the investigation for the development of a potential antifungal agent.

## Antimalarial, Antibacterial and Antiviral Activities

Rubiadin and RBME have been shown to have antimalarial activities with  $IC_{50}$  values of 13.00 and  $1.56 \mu\text{g}/\text{mL}$ , respectively.<sup>68</sup> The number of *Plasmodium falciparum*

parasites (schizonts) decreased significantly in a dose-dependent manner with almost a 100% of inhibition by RBME ( $30 \mu\text{g}/\text{mL}$ )<sup>69</sup> indicating that they have the potential to be developed as antiplasmodial agents. Rubiadin and RBME showed antibacterial activity against *Staphylococcus aureus* with MIC of 32–64 and  $>256 \mu\text{g}/\text{mL}$ , respectively. The mechanism of action seems to involve an increase in the levels of superoxide anion  $O_2^{\bullet-}$  and/or singlet molecular oxygen  $^1O_2$ .<sup>70</sup> In another study, Rubiadin was investigated against hepatitis B virus (HBV) using HepG2.2.15 cells. Rubiadin inhibited HBV DNA replication and lowered hepatitis B e antigen (HBeAg) as well as hepatitis B core antigen (HBcAg) levels. It also decreased HBV x (HBx) protein expression and reduced intracellular free calcium suggesting that it is a promising anti-HBV drug candidate (Figure 9).<sup>30</sup>

## Pharmacokinetics of Rubiadin

AQs which are absorbed mostly through the intestines and are primarily distributed in tissues and organs that receive good blood supply are transformed into another AQ, leading to potential pharmacological and/or toxicological effects.<sup>71</sup> The main components of *Morinda officinalis* are Rubiadin and RBME. To investigate the pharmacokinetics and tissue distribution of these two compounds in rat plasma and tissues, Shi et al<sup>17</sup> used an ultra-performance liquid chromatography-tandem mass spectrometry (UPLC-MS/MS). When compared to the findings from *Morinda officinalis* without wood (MO), the salt-processed *Morinda officinalis* (SMO) groups had significant increase in the maximum concentration (C<sub>max</sub>) and area under the curve (AUC<sub>0-t</sub>) indicating that salt steaming can increase Rubiadin's and RBME's bioavailabilities. Rubiadin had a time to maximum concentration (T<sub>max</sub>) of 1.5 h, which was longer than RBME, although RBME had the highest C<sub>max</sub>, particularly in the SMO extract. Additionally, the small intestine had the highest concentrations of both Rubiadin and RBME. Nevertheless, due to the limited study focus on Rubiadin's pharmacokinetic features, a comprehensive assessment of Rubiadin's absorption, distribution, metabolism and excretion profiles remains lacking.

## Absorption, Distribution, Metabolism, Excretion, and Toxicity (ADMET) Properties of Rubiadin

The variable nearest neighbor (vNN)-ADMET webserver was used to predict ADMET properties<sup>72</sup> of Rubiadin and to build new models based on vNN methodology. The parameters were classified as effects on the liver toxicity profile, metabolism, membrane transporters function, hERG (cardiotoxicity) activity, MMP (mitochondrial toxicity assay), mutagenicity (AMES test), and the maximum recommended therapeutic dose (MRTD). According to the unrestricted prediction model of the program, Rubiadin causes drug-induced liver injury (DILI) but not cytotoxicity, whereas the restricted model has no high confidence prediction. Rubiadin may produce positive findings for the human liver microsomal (HLM) stability assay and according to the unrestricted applicability domain, it may be rapidly metabolized. Rubiadin has the potential to inhibit the CYP 1A2, 2D6, 2C9, and 2C19 enzymes, but not the CYP 3A4 enzymes, as predicted by both models. Rubiadin has been found to have no effect on membrane transporters such as BBB and P-glycoprotein (P-gp).

Rubiadin causes mutations and may cause mitochondrial malfunction, according to the results of the AMES and MMP assays. The MRTD for Rubiadin was found to be 665 mg/day, as predicted by the software.

Apart from the parameters listed above, the toxicity estimation software tool (TEST) was used to estimate Rubiadin toxicity using quantitative structure-activity relationships (QSARs) approaches.<sup>73</sup> By employing TEST and QSAR techniques, the oral rat LD<sub>50</sub> mg/kg (predicted value) of Rubiadin was found to be 1307.13, 3502.50, and 487.82 mg/kg, respectively, to consensus method, hierarchical clustering technique, and nearest neighbor technique. There is a possibility that the mutagenicity assay will be positive, as shown by the software when all three QSAR techniques are used. According to the consensus approach, hierarchical clustering technique, and nearest neighbor technique, the predicted value of the mutagenicity assay was 0.98, 0.97, and 1.00, respectively.

## Molecular Docking of Rubiadin Against the Cancer Target Proteins

Molecular docking is a computational tool that can predict how a ligand will attach to a protein with a known three-dimensional structure. Docking may be used to do computer-generated screening on enormous collections of compounds, rate the outcomes, and offer structural models for in what manner the ligands inhibit the target, which is tremendously beneficial in the search for new inhibitors. There are no literature about molecular docking studies describing the interaction of Rubiadin with molecular targets involved in cancer development. To circumvent this constraint, we employed protein-ligand molecular docking to assess the Rubiadin's binding mechanism and interaction energy with four important enzyme targets, which were identified in this research as being responsible for variety of cancers.

A number of cancer treatments have been evaluated in clinical trials to see if they can inhibit the cMET receptor tyrosine kinase, and resistance mutations in the cMET gene are beginning to be identified in a number of these medications. Molecular investigations are still required to further understand individual cMET modifications at the molecular level, particularly in terms of small molecule identification.<sup>74</sup> In certain cancers, chromosomal translocation, amplification, or point mutations in the anaplastic lymphoma kinase (ALK) gene cause the tyrosine kinase to be constitutively activated. This gene has been found as a potential target for molecular docking studies, and it will be investigated extensively.<sup>75</sup> PI5P4Ks have



been shown to play a role in the growth of cancer cells as well as the development of other disorders. Due to a lack of effective and selective small drugs on the market, targeting these kinases for therapeutic purposes has gotten little attention.<sup>76</sup> Hsp90 and Hsp90 have been linked to cancer and neurological disorders, although determining their precise role in these diseases has been difficult due to a lack of specific pharmacological studies.<sup>77</sup> The protein with the PDB IDs 3AOX, 6OLX, 6OSP, and 6SDC were extracted from the protein data bank to commemorate the above four targets.

Molegro Virtual Docker (MVD) 6.0 was used to conduct the molecular docking study.<sup>78</sup> The docking procedure includes the following steps. MVD was used to import the molecules, including protein and ligand (Rubiadin). In the protein molecule, potential binding sites and the configuration of the search space were determined. The Docking Wizard was used to run a docking simulation. The Pose Organizer and the ligand energy inspector tool were used to inspect the docking results, and the results were tabulated and the docked view was extracted (Table 3). The MolDock score with the lowest values was discovered to have the highest binding affinity to the target proteins. Rubiadin affinity for cancer targets was found to be 6SDC>6OLX>3AOX>6OSP, according to the report obtained. This result strengthens the anticancer potential of Rubiadin and that could help to enlighten this biologically active compound to the next level of drug discovery and development.

## Cosmetic Formulation Containing Rubiadin

Rubiadin has been used as an active ingredient in a cream formulation conducted by a group of Korean researchers. The researchers reported that it had an excellent anti-allergy effect by inhibiting  $\beta$ -hexosaminidase secretion and the expression of caspase-1. The cream has been patented and relates to a cosmetic composition comprising ceramide, which can relieve atopic symptoms, additionally conferred by its moisturizing effect.<sup>79</sup>

## Possible Structural Modifications in Rubiadin

Currently, it remains unclear whether the bioactivities of Rubiadin can be improved via structural modifications. Some analogues of Rubiadin have been isolated or synthesized using methylation and acylation reactions, which are possible due to their phenolic hydroxyl groups. The side-chain modifications is an impetus for further efforts to

increase the therapeutic potential of this class of compounds (Figure 10). For example, Rubiadin analogues 1–3 have been synthesised and their cytotoxic activities against MCF-7 and K-562 cancer cell lines and the structure–activity relationship have been described.<sup>80</sup> The structure–activity relationship suggested that methoxy and hydroxyl groups are important for the cytotoxicity and selectivity of the substituted Aqs. Further RBME 4 and Rubiadin-3-methyl ether 5 were isolated from different medicinal plants and some of their biological activities were investigated (Table 1). Additionally, Rubiadin-1-methyl ether-3-O- $\beta$ -primeveroside 6 has been isolated, characterised and reported from *Pentas lanceolata*.<sup>81</sup>

The in silico design of more potent Rubiadin derivatives can be used as a way forward for novel drug discovery and development. Nevertheless, in vitro and in vivo studies should be conducted in future to confirm the safety and efficacy of all semi-synthetic derivatives of Rubiadin. Additionally, more studies relating to its structure–activity relationship (SAR) are warranted in the future to obtain several other novel compounds derived from Rubiadin.

## Conclusion and Future Perspectives

In this review, the presence of Rubiadin in medicinal plants and its isolation, synthesis, structural characterization, physicochemical properties, along with its biosynthesis are described in detail. Additionally, the scientific updates on its biological and therapeutic potentials have been provided. Accumulating evidence provided by various preclinical studies has shown that Rubiadin can be a promising anticancer, anti-osteoporotic, hepatoprotective, neuroprotective, anti-inflammatory, antidiabetic, antioxidant, antibacterial, antimalarial, antifungal and antiviral drug candidate for further development. Rubiadin was proven to have the highest binding affinity to the cancer targeted proteins in an in silico study, thus we believe it may be a potential anticancer molecule. The in silico findings indicate that Rubiadin has a high ligand-potentiality for a wide range of macromolecules, leading us to believe that it may interact with a variety of other enzymes or proteins that were not included in this simulation. It is hoped that this review will stimulate further investigations on Rubiadin in relation to its pharmacokinetics, pharmacodynamics, clinical and SAR studies, which can help accelerate the development and utilization of Rubiadin as a promising drug candidate in the near future.

**Table 3** Docked Study Results of Rubiadin with the Cancer Target Proteins

S. No.	Protein	Ligand	MolDock Score	Rerank Score	HBond	Amino Acid Residue ID	Docked View
1.	3AOX	Rubiadin	-76.1811	-76.5953	-5.47821	Ala 1148, Ala 1200, Asp 1203, Glu 1197, Gly 1123, Gly 1202, Gly 1269, Leu 1122, Leu 1196, Leu 1198, Leu 1256, Lys 1150, Met 1199, Val 1130, Val 1180, water 60, 77, 121, 149, 175.	
2.	6OLX	Rubiadin	-87.933	-89.7029	-2.5	Ala 111, Asn 51, Gly 135, Leu 103, Leu 107, Met 98, Phe 22, Phe 138, Trp 162, Tyr 139, Val 136, Val 150, water 34, 55, 82, 89, 112, 132, 141, 161, 179, 180, 266, 307, 336, 347.	

3.	6OSP	Rubiadin	-72.1067	-66.5032	-3.53132	<p>Arg 197, Asp 151, Asp 359, Gin 177, His 363, Ile 143, Ile 147, Ile 194, Ile 357, Ile 358, Ile 360, Leu 361, Lys 145, Phe 178, Pro 176, Thr 196, Val 199.</p>	
4.	6SDC	Rubiadin	-96.0669	-78.6787	-2.9185	<p>Ala 1221, Asp 1222, Glu 1127, Gly 1128, Gly 1224, His 1202, Ile 1130, Leu 1140, Leu 1157, Leu 1195, Lys 1110, Met 1131, Phe 1134, Phe 1200, Phe 1223, Val 1139, Val 1220, water 24, 38, 86, 195, 227, 259.</p>	

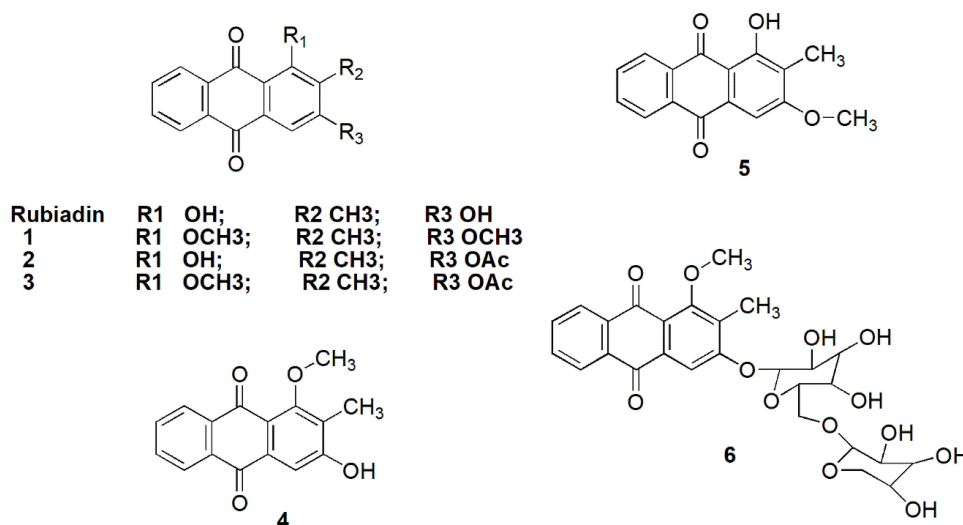


**Figure 10** Possible structural modifications of Rubiadin.  
**Note:** Created with ChemDraw Ultra 8.0.

## Consent for Publication

The final version of the manuscript was reviewed by all the authors who consented to its submission.

## Acknowledgments

The authors acknowledge AIMST University, Kedah, Malaysia, and Universiti Kuala Lumpur Royal College of Medicine Perak, Ipoh, Perak, Malaysia, for providing the facilities and services required to complete the study. The figures and graphical abstract in this manuscript were created with BioRender.com and the support of <https://biorender.com> under a paid subscription.

## Author Contributions

All the authors made substantial contributions to conception and design, acquisition of data, or analysis and interpretation of data; took part in drafting the article or revising it critically for important intellectual content; agreed to submit to the current journal; gave final approval of the version to be published; and agree to be accountable for all aspects of the work.

## Funding

There is no funding to report.

## Disclosure

The authors have no conflict of interest associated with the publication and report no conflicts of interest for this work. There was also no significant financial support for this work.

## References

- Duval J, Pecher V, Poujol M, Lesellier E. Research advances for the extraction, analysis and uses of anthraquinones: a review. *Ind Crops Prod.* 2016;94:812–833. doi:10.1016/j.indcrop.2016.09.056
- Seigler DS. Benzoquinones, naphthoquinones, and anthraquinones. In: *Plant Secondary Metabolism*. Springer; 1998.
- Dave H, Ledwani L. A review on anthraquinones isolated from Cassia species and their applications. *Indian J Natl Prod Resources.* 2012;3(2012):291–319.
- Malik EM, Müller CE. Anthraquinones as pharmacological tools and drugs. *Med Res Rev.* 2016;36(4):705–748. doi:10.1002/med.21391
- Huang Q, Lu G, Shen HM, Chung MC, Ong CN. Anti-cancer properties of anthraquinones from rhubarb. *Med Res Rev.* 2007;27(5):609–630. doi:10.1002/med.20094
- Murdock K, Child R, Fabio P, et al. Antitumor agents. 1. 1, 4-Bis [(aminoalkyl) amino]-9, 10-anthracenediones. *J Med Chem.* 1979;22(9):1024–1030. doi:10.1021/jm00195a002
- Shrestha JP, Fosso MY, Bearss J, Chang C-WT. Synthesis and anticancer structure activity relationship investigation of cationic anthraquinone analogs. *Eur J Med Chem.* 2014;77:96–102. doi:10.1016/j.ejmech.2014.02.060
- Shrestha JP, Subedi YP, Chen L, Chang C-WT. A mode of action study of cationic anthraquinone analogs: a new class of highly potent anticancer agents. *MedChemComm.* 2015;6(11):2012–2022. doi:10.1039/C5MD00314H
- Chien S-C, Wu Y-C, Chen Z-W, Yang W-C. Naturally occurring anthraquinones: chemistry and therapeutic potential in autoimmune diabetes. *Evid Based Complement Altern Med.* 2015;2015:1–13. doi:10.1155/2015/357357
- Khan K, Karodi R, Siddiqui A, Thube S, Rub R. Development of anti-acne gel formulation of anthraquinones rich fraction from *Rubia cordifolia* (Rubiaceae). *Int J Appl Res Nat Prod.* 2011;4(4):28–36.
- Davis RH, Agnew PS, Shapiro E. Antiarthritic activity of anthraquinones found in aloe vera for podiatric medicine. *J Am Podiatr Med Assoc.* 1986;76(2):1–8.
- Wuthi-udomlert M, Kupittayanant P, Gritsanapan W. In vitro evaluation of antifungal activity of anthraquinone derivatives of *Senna alata*. *J Health Res.* 2010;24(3):117–122.

13. Fosso MY, Chan KY, Gregory R, Chang C-WT. Library synthesis and antibacterial investigation of cationic anthraquinone analogs. *ACS Comb Sci*. 2012;14(3):231–235. doi:10.1021/co2002075
14. Winter R, Cornell KA, Johnson LL, Ignatushchenko M, Hinrichs DJ, Riscoe MK. Potentiation of the antimalarial agent rufigallol. *Antimicrob Agents Chemother*. 1996;40(6):1408–1411. doi:10.1128/AAC.40.6.1408
15. Tikhomirov AS, Shtil AA, Shchekotikhin AE. Advances in the discovery of anthraquinone-based anticancer agents. *Recent Pat Anticancer Drug Discov*. 2018;13(2):159–183. doi:10.2174/1574892813666171206123114
16. Rao GMM, Rao CV, Pushpangadan P, Shirwaikar A. Hepatoprotective effects of rubiadin, a major constituent of *Rubia cordifolia* Linn. *J Ethnopharmacol*. 2006;103(3):484–490. doi:10.1016/j.jep.2005.08.073
17. Shi J, Ren X, Wang J, Wei X, Liu B, Jia T. Effects of the salt-processing method on the pharmacokinetics and tissue distribution of orally administered *Morinda officinalis* how. *Extract J Analyt Methods Chem*. 2020;2020:1–11.
18. Patel V, Patel R. Simultaneous analysis and quantification of markers of manjisthadi churna using high performance thin layer chromatography. *Indian J Pharm Sci*. 2013;75(1):106. doi:10.4103/0250-474X.113541
19. Zhang J, Zhang Z, Bao J, et al. Jia-Jian-Di-Huang-Yin-Zi decoction reduces apoptosis induced by both mitochondrial and endoplasmic reticulum caspase12 pathways in the mouse model of Parkinson's disease. *J Ethnopharmacol*. 2017;203:69–79. doi:10.1016/j.jep.2016.12.053
20. Qin L, Han T, Zhang Q, et al. Antiosteoporotic chemical constituents from Er-Xian Decoction, a traditional Chinese herbal formula. *J Ethnopharmacol*. 2008;118(2):271–279. doi:10.1016/j.jep.2008.04.009
21. Bhatt P, Kushwah A. *Rubia cordifolia* overview: a new approach to treat cardiac disorders. *Int J Drug Dev Res*. 2013;5(2):47–54.
22. Ojha JK, Dwivedi KN, Chaurasiya AK. Effect of *Rubia cordifolia* on non healing diabetic foot ulcer. *Nat Sem Trad Med Plants Skin Care*. 1994:17.
23. Gogate VU, Ramkrishnan S (editor). *Ayurvedic Pharmacology and Therapeutic Uses of Medicinal Plants (Dravya-gunavignyan)*. Mumbai: Swami Prakashananda Ayurveda Research Centre; 2000.
24. Lodia S, Kansala L. Antioxidant activity of *Rubia cordifolia* against lead toxicity. *Int J Pharma Sci Res*. 2012;3(7):2224.
25. Tripathi YB, Singh AV. Role of *Rubia cordifolia* Linn. in radiation protection. *Future Med Chem*. 2007;12(7):627–644.
26. Karodi R, Jadhav M, Rub R, Bafna A. Evaluation of the wound healing activity of a crude extract of *Rubia cordifolia* L. (Indian madder) in mice. *Int J Appl Res Nat Prod*. 2009;2(2):12–18.
27. Prajapati SN, Parmar KA. Anti-viral and in-vitro free radical scavenging activity of leaves of *Rubia cordifolia*. *Int J Phytomed*. 2011;3(1):98.
28. Tripathi Y, Sharma M, Manickam M. Rubiadin, a new antioxidant from *Rubia cordifolia*. *Indian J Biochem Biophys*. 1997;34(3):302–306.
29. Takano T, Kondo T, Nakatsubo F. Facile synthesis of rubiadin by microwave heating. *J Wood Sci*. 2006;52(1):90–92. doi:10.1007/s10086-005-0727-6
30. Peng Z, Fang G, Peng F, et al. Effects of Rubiadin isolated from *Prismatomeris connata* on anti-hepatitis B virus activity in vitro. *Phytother Res*. 2017;31(12):1962–1970. doi:10.1002/ptr.5945
31. National Center for Biotechnology Information. PubChem compound summary for CID 124062, Rubiadin. Available from: <https://pubchem.ncbi.nlm.nih.gov/compound/Rubiadin>. Accessed October 20, 2021.
32. Lipinski CA, Lombardo F, Dominy BW, Feeney PJ. Experimental and computational approaches to estimate solubility and permeability in drug discovery and development settings. *Adv Drug Deliv Rev*. 1997;23(1–3):3–25. doi:10.1016/S0169-409X(96)00423-1
33. Zhang M-Q, Wilkinson B. Drug discovery beyond the 'rule-of-five'. *Curr Opin Biotechnol*. 2007;18(6):478–488. doi:10.1016/j.copbio.2007.10.005
34. Shukla V, Asthana S, Gupta P, Dwivedi PD, Tripathi A, Das M. Toxicity of naturally occurring anthraquinones. In: *Advances in Molecular Toxicology*. Vol. 11. Elsevier; 2017.
35. Verma A, Mahalwal V, Kumar B. Antiepileptic activity of rubiadin isolated from the roots of *Rubia cordifolia* in mice. *Int J Pharma Sci Res*. 2019;10:3022–3028.
36. Tian W, Wang C, Li D, Hou H. Novel anthraquinone compounds as anticancer agents and their potential mechanism. *Future Med Chem*. 2020;12(7):627–644.
37. Cogno IS, Gilardi P, Comini L, Núñez-Montoya SC, Cabrera JL, Rivarola VA. Natural photosensitizers in photodynamic therapy: in vitro activity against monolayers and spheroids of human colorectal adenocarcinoma SW480 cells. *Photodiagnosis Photodyn Ther*. 2020;31:101852. doi:10.1016/j.pdpdt.2020.101852
38. Comini L, Fernandez I, Vittar NR, Montoya SN, Cabrera J, Rivarola V. Photodynamic activity of anthraquinones isolated from *Heterophyllaea pustulata* Hook f. (Rubiaceae) on MCF-7c3 breast cancer cells. *Phytomedicine*. 2011;18(12):1093–1095. doi:10.1016/j.phymed.2011.05.008
39. Vittar NBR, Comini L, Fernandez IM, et al. Photochemotherapy using natural anthraquinones: Rubiadin and Soranjidiol sensitize human cancer cell to die by apoptosis. *Photodiagnosis Photodyn Ther*. 2014;11(2):182–192. doi:10.1016/j.pdpdt.2014.02.002
40. Chiou C-T, Hsu R-Y, Lin L-C. Isolation and cytotoxic effect of anthraquinones from *Morinda umbellata*. *Planta Med*. 2014;80(13):1113–1117. doi:10.1055/s-0034-1382956
41. Ali A, Ismail N, Mackeen M, et al. Antiviral, cytotoxic and antimicrobial activities of anthraquinones isolated from the roots of *Morinda elliptica*. *Pharm Biol*. 2000;38(4):298–301. doi:10.1076/1388-0209(200009)38:4;1-A:FT298
42. Kanokmedhakul K, Kanokmedhakul S, Phatchana R. Biological activity of anthraquinones and triterpenoids from *prismatomeris fragrans*. *J Ethnopharmacol*. 2005;100(3):284–288. doi:10.1016/j.jep.2005.03.018
43. Inoue K, Yoshida M, Takahashi M, et al. Possible contribution of rubiadin, a metabolite of madder color, to renal carcinogenesis in rats. *Food Chem Toxicol*. 2009;47(4):752–759. doi:10.1016/j.fct.2009.01.003
44. Inoue K, Yoshida M, Takahashi M, et al. Carcinogenic potential of alizarin and rubiadin, components of madder color, in a rat medium-term multi-organ bioassay. *Cancer Sci*. 2009;100(12):2261–2267. doi:10.1111/j.1349-7006.2009.01342.x
45. Blömeke B, Poginsky B, Schmutte C, Marquardt H, Westendorf J. Formation of genotoxic metabolites from anthraquinone glycosides, present in *Rubia tinctorum* L. *Mutat Res/Fundament Mol Mechan Mutagen*. 1992;265(2):263–272. doi:10.1016/0027-5107(92)90055-7
46. Siewert B, Stuppner H. The photoactivity of natural products—an overlooked potential of phytomedicines? *Phytomedicine*. 2019;60:152985. doi:10.1016/j.phymed.2019.152985
47. Montoya SCN, Comini LR, Vittar BR, Fernández IM, Rivarola VA, Cabrera JL. Phototoxic effects of *Heterophyllaea pustulata* (Rubiaceae). *Toxicol*. 2008;51(8):1409–1415. doi:10.1016/j.toxicol.2008.03.011
48. Micheloud JF, Colque-Caro LA, Comini LR, et al. Spontaneous photosensitization by *Heterophyllaea pustulata* Hook. f. (Rubiaceae), in sheep from Northwestern Argentina. *Trop Anim Health Prod*. 2017;49(7):1553–1556. doi:10.1007/s11250-017-1354-0
49. Micheloud JF, Aguirre LS, Marioni J, et al. Experimental poisoning by *Heterophyllaea pustulata* Hook. f. (Rubiaceae) in goats. Clinical, biochemical and toxicological aspects. *Toxicol*. 2019;165:56–61. doi:10.1016/j.toxicol.2019.04.015

50. Sambrook P, Cooper C. Osteoporosis. *Lancet*. 2006;367(9527):2010–2018. doi:10.1016/S0140-6736(06)68891-0
51. He Y-Q, Zhang Q, Shen Y, et al. Rubiadin-1-methyl ether from *Morinda officinalis* How. Inhibits osteoclastogenesis through blocking RANKL-induced NF- $\kappa$ B pathway. *Biochem Biophys Res Commun*. 2018;506(4):927–931. doi:10.1016/j.bbrc.2018.1.0100
52. Bao L, Qin L, Liu L, et al. Anthraquinone compounds from *Morinda officinalis* inhibit osteoclastic bone resorption in vitro. *Chem Biol Interact*. 2011;194(2–3):97–105. doi:10.1016/j.cbi.2011.08.013
53. Wu Y-B, Zheng C-J, Qin L-P, et al. Antiosteoporotic activity of anthraquinones from *Morinda officinalis* on osteoblasts and osteoclasts. *Molecules*. 2009;14(1):573–583. doi:10.3390/molecules14010573
54. Xia T, Dong X, Lin L, et al. Metabolomics profiling provides valuable insights into the underlying mechanisms of *Morinda officinalis* on protecting glucocorticoid-induced osteoporosis. *J Pharm Biomed Anal*. 2019;166:336–346. doi:10.1016/j.jpba.2019.01.019
55. Libby P. Inflammatory mechanisms: the molecular basis of inflammation and disease. *Nutr Rev*. 2007;65(suppl\_3):S140–S146. doi:10.1301/nr.2007.dec.S140-S146
56. Mohr ETB, Dos Santos Nascimento MVP, da Rosa JS, et al. Evidence that the anti-inflammatory effect of Rubiadin-1-methyl ether has an immunomodulatory context. *Mediators Inflamm*. 2019;2019:1–12. doi:10.1155/2019/6474168
57. Mujeeb M, Ahad A, Aqil M, et al. Ameliorative effect of rubiadin-loaded nanocarriers in STZ-NA-induced diabetic nephropathy in rats: formulation optimization, molecular docking, and in vivo biological evaluation. *Drug Deliv Transl Res*. 2021;1–14. doi:10.1007/s13346-021-00971-0
58. Yen G-C, Duh P-D, Chuang D-Y. Antioxidant activity of anthraquinones and anthrone. *Food Chem*. 2000;70(4):437–441. doi:10.1016/S0308-8146(00)00108-4
59. Malterud KE, Farbrot TL, Huse AE, Sund RB. Antioxidant and radical scavenging effects of anthraquinones and anthrones. *Pharmacology*. 1993;47(Suppl. 1):77–85. doi:10.1159/000139846
60. Baghiani A, Charef N, Djarmouni M, Saadeh A, Arrar L, Mubarak S. Free radical scavenging and antioxidant effects of some anthraquinone derivatives. *Med Chem (Los Angeles)*. 2011;7(6):639–644. doi:10.2174/157340611797928424
61. Tripathi Y, Sharma M. Comparison of the antioxidant action of the alcoholic extract of *Rubia cordifolia* with rubiadin. *Indian J Biochem Biophys*. 1998;35(5):313–316.
62. Mishra BB, Kishore N, Tiwari VK, Singh DD, Tripathi V. A novel antifungal anthraquinone from seeds of *Aegle marmelos* Correa (family Rutaceae). *Fitoterapia*. 2010;81(2):104–107. doi:10.1016/j.fitote.2009.08.009
63. Mohamadzadeh M, Zarei M, Vessal M. Synthesis, in vitro biological evaluation and in silico molecular docking studies of novel  $\beta$ -lactam-anthraquinone hybrids. *Bioorg Chem*. 2020;95:103515. doi:10.1016/j.bioorg.2019.103515
64. Khan MS, Gao J, Chen X, et al. The endophytic bacteria *Bacillus velezensis* Lle-9, isolated from *Lilium leucanthum*, harbors antifungal activity and plant growth-promoting effects. *J Microbiol Biotechnol*. 2020;30(5):668–680. doi:10.4014/jmb.1910.10021
65. Marioni J, Da Silva MA, Cabrera JL, Montoya SCN, Paraje MG. The anthraquinones rubiadin and its 1-methyl ether isolated from *Heterophyllaea pustulata* reduces *Candida tropicalis* biofilms formation. *Phytomedicine*. 2016;23(12):1321–1328. doi:10.1016/j.phymed.2016.07.008
66. Marioni J, Bresolí-Obach R, Agut M, et al. On the mechanism of *Candida tropicalis* biofilm reduction by the combined action of naturally-occurring anthraquinones and blue light. *PLoS One*. 2017;12(7):e0181517. doi:10.1371/journal.pone.0181517
67. Montoya SCN, Comini LR, Sarmiento M, et al. Natural anthraquinones probed as type I and type II photosensitizers: singlet oxygen and superoxide anion production. *J Photochem Photobiol B*. 2005;78(1):77–83. doi:10.1016/j.jphotobiol.2004.09.009
68. Likhitwitayawuid K, Dej-adisai S, Jongbunprasert V, Krungkrai J. Antimalarials from *Stephania venosa*, *Prismatomeris sessiliflora*, *Diospyros Montana* and *Murraya siamensis* L. *Planta Med*. 1999;65(08):754–756. doi:10.1055/s-2006-960858
69. Koumaglo K, Gbeassor M, Nikabu O, De Souza C, Werner W. Effects of three compounds extracted from *Morinda lucida* on *Plasmodium falciparum*. *Planta Med*. 1992;58(06):533–534. doi:10.1055/s-2006-961543
70. Comini L, Montoya SN, Páez P, Argüello GA, Albesa I, Cabrera J. Antibacterial activity of anthraquinone derivatives from *Heterophyllaea pustulata* (Rubiaceae). *J Photochem Photobiol B*. 2011;102(2):108–114. doi:10.1016/j.jphotobiol.2010.09.009
71. Wang D, Wang X-H, Yu X, et al. Pharmacokinetics of anthraquinones from medicinal plants. *Front Pharmacol*. 2021;12:306.
72. Schyman P, Liu R, Desai V, Wallqvist A. vNN web server for ADMET predictions. *Front Pharmacol*. 2017;8:889. doi:10.3389/fphar.2017.00889
73. EPA. User's guide for T.E.S.T. (version 5.1) (toxicity estimation software tool): a program to estimate toxicity from molecular structure. Available from: <https://www.epa.gov/chemical-research/toxicity-estimation-software-tool-test>. Accessed October 20, 2021.
74. Collie GW, Koh CM, O'Neill DJ, et al. Structural and molecular insight into resistance mechanisms of first generation cMET inhibitors. *ACS Med Chem Lett*. 2019;10(9):1322–1327. doi:10.1021/acsmchemlett.9b00276
75. Sakamoto H, Tsukaguchi T, Hiroshima S, et al. CH5424802, a selective ALK inhibitor capable of blocking the resistant gatekeeper mutant. *Cancer Cell*. 2011;19(5):679–690. doi:10.1016/j.ccr.2011.04.004
76. Sivakumaren SC, Shim H, Zhang T, et al. Targeting the PI5P4K lipid kinase family in cancer using covalent inhibitors. *Cell Chem Biol*. 2020;27(5):525–537. doi:10.1016/j.chembiol.2020.02.003
77. Huck JD, Que NL, Sharma S, Taldone T, Chiosis G, Gewirth DT. Structures of Hsp90 $\alpha$  and Hsp90 $\beta$  bound to a purine-scaffold inhibitor reveal an exploitable residue for drug selectivity. *Proteins Struct Func Bioinform*. 2019;87(10):869–877. doi:10.1002/prot.25750
78. Thomsen R, Christensen MH. MolDock: a new technique for high-accuracy molecular docking. *J Med Chem*. 2006;49(11):3315–3321. doi:10.1021/jm051197e
79. Cosmetic components comprised of the rubiadin having anti-allergic activity. Patent number KR101337564B1. Korea Kolmar Co., Ltd.; 2010. Available from: <https://patents.google.com/patent/KR101337564B1/en>. Accessed October 28, 2021.
80. Akhtar MN, Zareen S, Yeap SK, et al. Total synthesis, cytotoxic effects of damnacanthal, nordamnacanthal and related anthraquinone analogues. *Molecules*. 2013;18(8):10042–10055. doi:10.3390/molecules180810042
81. Kumar P, Sharma AK, Shukla P. Physicochemical screening of marker anthraquinones and derivatives from the *Pentas lanceolata* (Forss. k.) deflers leaves. *Eur J Pharm Med Res*. 2017;4(5):439–446.
82. Dosseh C, Tessier A, Delaveau P. Nouvelles Quinones des Racines de *Rubia cordifolia* L., III. *Planta Med*. 1981;43(12):360–366. doi:10.1055/s-2007-971524
83. Shen C-H, Liu C-T, Song X-J, et al. Evaluation of analgesic and anti-inflammatory activities of *Rubia cordifolia* L. by spectrum-effect relationships. *J Chromatogr B*. 2018;1090:73–80. doi:10.1016/j.jchromb.2018.05.021
84. Liu Q, Kim SB, Ahn JH, Hwang BY, Kim SY, Lee MK. Anthraquinones from *Morinda officinalis* roots enhance adipocyte differentiation in 3T3-L1 cells. *Nat Prod Res*. 2012;26(18):1750–1754. doi:10.1080/14786419.2011.608676

85. Zhang J-H, Xin H-L, Xu Y-M, et al. Morinda officinalis How.—a comprehensive review of traditional uses, phytochemistry and pharmacology. *J Ethnopharmacol.* 2018;213:230–255. doi:10.1016/j.jep.2017.10.028
86. Zhao X, Wei J, Yang M. Simultaneous analysis of iridoid glycosides and anthraquinones in Morinda officinalis using UPLC-QqQ-MS/MS and UPLC-Q/TOF-MSE. *Molecules.* 2018;23(5):1070. doi:10.3390/molecules23051070
87. Mugas ML, Marioni J, Martinez F, et al. Inactivation of herpes simplex virus by photosensitizing anthraquinones isolated from heterophyllaea pustulata. *Planta Med.* 2021;80:716–723.
88. Schunck HE. III. On rubian and its products of decomposition. *Philos Transact Royal Soc London.* 1853;(143):67–107. doi:10.1098/rstl.1853.0003
89. Kawasaki Y, Goda Y, Yoshihira K. The mutagenic constituents of Rubia tinctorum. *Chem Pharm Bull (Tokyo).* 1992;40(6):1504–1509. doi:10.1248/cpb.40.1504
90. Cuoco G, Mathe C, Archier P, Chemat F, Vieillescazes C. A multivariate study of the performance of an ultrasound-assisted madder dyes extraction and characterization by liquid chromatography-photodiode array detection. *Ultrason Sonochem.* 2009;16(1):75–82. doi:10.1016/j.ulsonch.2008.05.014
91. Cooksey C. Quirks of dye nomenclature. 14. Madder: queen of red dyes. *Biotech Histochem.* 2020;95(6):474–482. doi:10.1080/10520295.2020.1714079
92. Tuntiwachwuttikul P, Butsuri Y, Sukkoet P, Prawat U, Taylor WC. Anthraquinones from the roots of Prismaticomeris malayana. *Nat Prod Res.* 2008;22(11):962–968. doi:10.1080/14786410701650261
93. Rahman MM. Evaluation of Hymenodictyon excelsum phytochemical's therapeutic value against prostate cancer by molecular Docking study. *Jundishapur j Nat Pharma Prod.* 2015;10(1). doi:10.17795/jjnpp-18216
94. Ahmad R, Shaari K, Lajis NH, Hamzah AS, Ismail NH, Kitajima M. Anthraquinones from Hedyotis capitellata. *Phytochemistry.* 2005;66(10):1141–1147. doi:10.1016/j.phytochem.2005.02.023
95. Usai M, Marchetti M. Anthraquinone distribution in the hypogean apparatus of Rubia peregrina L. growing wild in Sardinia. *Nat Prod Res.* 2010;24(7):626–632. doi:10.1080/14786410902884842
96. Bussmann RW, Hennig L, Giannis A, Ortwein J, Kutchan TM, Feng X. Anthraquinone content in Noni (Morinda citrifolia L.). *Evid Based Complement Altern Med.* 2013;2013:1–5. doi:10.1155/2013/208378
97. Rajan R, Venkataraman R, Baby S. A new lupane-type triterpenoid fatty acid ester and other isolates from Ophiorrhiza shendurunii. *Nat Prod Res.* 2016;30(19):2197–2203. doi:10.1080/14786419.2016.1160232
98. Osman CP, Ismail NH, Ahmad R, Ahmat N, Awang K, Jaafar FM. Anthraquinones with antiplasmodial activity from the roots of Rennellia elliptica Korth. (Rubiaceae). *Molecules.* 2010;15(10):7218–7226. doi:10.3390/molecules15107218
99. Yuan S, Zhao Y. Chemical constituents of Knoxia valerianoides. *Acta Pharmaceutica Sinica.* 2006;41(8):735–737.
100. Yoo NH, Jang DS, Lee YM, et al. Anthraquinones from the roots of Knoxia valerianoides inhibit the formation of advanced glycation end products and rat lens aldose reductase in vitro. *Arch Pharm Res.* 2010;33(2):209–214. doi:10.1007/s12272-010-0204-7
101. Zhao F, Wang S-J, Lin S, et al. Anthraquinones from the roots of Knoxia valerianoides. *J Asian Nat Prod Res.* 2011;13(11):1023–1029. doi:10.1080/10286020.2011.606813
102. Lan M, Luo C, Tan C, Chen L, Wei S, Zhu D. Study on chemical constituents of the ethyl acetate extract from Blumea aromatica. *J Chin Med Mater.* 2012;35(2):229–231.
103. Jiang J-S, Feng Z-M, Zhang P-C. Chemical constituents from root of Prismaticomeris tetrandra. *China J Chin Materia Medica.* 2005;30(22):1751–1753.
104. Huang W, Li Y, Jiang J. Chemical constituents from Hedyotis diffusa. *China J Chin Materia Medica.* 2009;34(6):712–714.
105. Liu G, Chen Z, Yao T, Ding W. Studies on the chemical constituents of Rhynchotechum vestitum Hook. F. et Thoms. *Acta Pharmaceutica Sinica.* 1990;25(9):699–704.
106. Haque MA, Khan G, Razzaque S, Khatun K, Chakraborty AK, Alam MS. Extraction of rubiadin dye from Swietenia mahagoni and its dyeing characteristics onto silk fabric using metallic mordants. *Indian J Fibre Text Res.* 2013;38:280–284.
107. Li S, Ouyang Q, Tan X, Shi S, Yao Z. Chemical constituents of Morinda officinalis how. *China J Chin Materia Medica.* 1991;16(11):675–676, 703.
108. Chokchaisiri S, Siriwananathien Y, Thongbamrer C, Suksamrarn A, Rukachaisirikul T. Morindaquinone, a new bianthraquinone from Morinda coreia roots. *Nat Prod Res.* 2019;1–7. doi:10.1080/14786419.2019.1705820
109. Zou X, Liang J, Ding L-S, Peng S-L. Studies on chemical constituents of Paederia scandense. *China J Chin Materia Medica.* 2006;31(17):1436–1441.
110. Li Y, Qi S, Chen X, Hu Z. Separation and determination of the anthraquinones in Xanthophyllum attopvensis pierre by nonaqueous capillary electrophoresis. *Talanta.* 2005;65(1):15–20.
111. Tosa H, Inuma M, Asai F, et al. Anthraquinones from Neonauclea calycina and their inhibitory activity against DNA topoisomerase II. *Biol Pharm Bull.* 1998;21(6):641–642. doi:10.1248/bpb.21.641
112. Khanh PN, Huong TT, Spiga O, et al. In silico screening of anthraquinones from Prismaticomeris memecyloides as novel phosphodiesterase type-5 inhibitors (PDE-5Is). *Revista Internacional De Andrologia.* 2018;16(4):147–158. doi:10.1016/j.androl.2017.07.001
113. Chen -R-R, Liu J, Chen Z, Cai W-J, Li X-F, Lu C-L. Anthraquinones extract from morinda angustifolia roxb. Root alleviates hepatic injury induced by carbon tetrachloride through inhibition of hepatic oxidative stress. *Evid Based Complement Altern Med.* 2020;2020. doi:10.1155/2020/9861571
114. Lv Z, Zhang Q, Chen R, Yu D. Alkaloids and anthraquinones from branches and leaves of Uvaria kurzii. *China J Chin Materia Medica.* 2011;36(9):1190–1192.

## Drug Design, Development and Therapy

### Publish your work in this journal

Drug Design, Development and Therapy is an international, peer-reviewed open-access journal that spans the spectrum of drug design and development through to clinical applications. Clinical outcomes, patient safety, and programs for the development and effective, safe, and sustained use of medicines are a feature of the journal, which has also

been accepted for indexing on PubMed Central. The manuscript management system is completely online and includes a very quick and fair peer-review system, which is all easy to use. Visit <http://www.dovepress.com/testimonials.php> to read real quotes from published authors.

Submit your manuscript here: <https://www.dovepress.com/drug-design-development-and-therapy-journal>